NSF/CEE-84031

PB85-132165

REPORT NO. CCEER-84-3

INELASTIC STATIC AND DYNAMIC ANALYSIS OF SHORT R/C BRIDGES SUBJECTED TO LATERAL LOADS

by

Mehdi Saiidi
James D. Hart
Bruce M. Douglas

A Report to the
National Science Foundation
Research Grant CEE-8108124

Civil Engineering Department
University of Nevada Reno

July 1984

50272-101

REPORT DOCUMENTATION PAGE	1. REPORT NO. NSF/CEE-84031	2.	3. Recipient's Accession No.
4. Title and Subtitle: Inelastic Static and Dynamic Analysis of Short R/C Bridges Subjected to Lateral Loads			5. Report Date: July 1984
			6.
7. Author(s): M. Saiidi, J.D. Hart, B.M. Douglas			8. Performing Organization Rept. No. CCEER-84-3
9. Performing Organization Name and Address: University of Nevada at Reno, Department of Civil Engineering, Reno, NV 89557			10. Project/Task/Work Unit No.
			11. Contract(C) or Grant(G) No. (C) (G) CEE8108124
12. Sponsoring Organization Name and Address: Directorate for Engineering (ENG), National Science Foundation, 1800 G Street, N.W., Washington, DC 20550			13. Type of Report & Period Covered
			14.

15. Supplementary Notes

16. Abstract (Limit: 200 words)

A multi-degree-of-freedom nonlinear analytical model is developed for response analysis of highway bridges subjected to lateral static loads, free vibration, and earthquake motions. Translational and rotational springs are incorporated at pier foundations, bases, and abutments to account for nonlinear effects; the deck and piers are treated as line elements. The Ramberg-Osgood model and the TQ-Hyst model are used to represent the cyclic behavior of the nonlinear components. The analytical model is used to determine the static and free vibration response of a bridge in Nevada. A reasonably good correlation between the calculated and measured results is achieved. The model is also used to evaluate the seismic performance of the bridge in accordance with recently developed Applied Technology Council Guidelines. The bridge performed well in resisting the loads specified by the seismic code used in its design.

17. Document Analysis a. Descriptors

Bridges
Mathematical models
Earthquake resistant structures
Loads (forces)
Static loads
Dynamic structural analysis

b. Identifiers/Open-Ended Terms

Nevada
B.M. Douglas, /PI

c. COSATI Field/Group

18. Availability Statement	19. Security Class (This Report)	21. No. of Pages
NTIS		104
	20. Security Class (This Page)	22. Price

(See ANSI-Z39.18) See Instructions on Reverse OPTIONAL FORM 272 (4-77) (Formerly NTIS-35) Department of Commerce

ABSTRACT

A multi-degree-of-freedom nonlinear analytical model for response analysis of highway bridges subjected to lateral static loads, free vibration, and earthquake motions is presented. The nonlinear effects are accounted for by incorporating translational and rotational springs at abutments, pier foundations, and at the base of piers. The deck and piers are treated as line elements.

Two hysteresis models are used to represent the cyclic behavior of the nonlinear components: the Ramberg-Osgood model (for abutment springs) and the TQ-Hyst model (for pier and foundation springs). The latter is a modified version of a previously developed model called Q-Hyst.

The analytical model is used to determine the static and free vibration response of a bridge in Northern Nevada (Rose Creek Interchange). The calculated results are compared with the measured values to evaluate the idealizations and the assumptions made in the model. A reasonably good correlation between the calculated and measured results is noted. It is pointed out that, due to lack of data for bridges with extensive nonlinearity, the correlation studies could be done only for small loads producing a limited degree of nonlinearity.

Finally, the model is used to evaluate the seismic performance of the Rose Creek Bridge based on the recently developed Applied Technology Council Guidelines for the seismic design of highway bridges and by analyzing the bridge for a variety of input earthquake records with different peak accelerations. It is shown that the Rose Creek Bridge performed well in resisting the loads specified by the seismic code used in the design of the bridge.

ACKNOWLEDGMENTS

The study presented in this report was part of a continuing study at the University of Nevada, Reno on the seismic response of highway bridges and was supported by the National Science Foundation Grant CEE-81Ø8124. The statements in this report are those of the authors and do not necessarily present the views of the National Science Foundation.

The authors are grateful to Mr. Al Stone, the Director of the Nevada Department of Transportation (NDOT), and Mr. Jim Dodson, chief Bridge Engineer at NDOT, for their cooperation in the course of this study.

Dr. Gary Norris, an associate professor of Civil Engineering at the University of Nevada Reno (UNR), is thanked for providing the stiffness properties of the pile foundations and for his valuable discussions about the foundation behavior. Mr. Jim Richardson, a graduate student of Civil Engineering at UNR, is thanked for providing the digitized measured data for the Rose Creek Bridge.

Miss Thelma "Jeanie" Pratt is especially thanked for her careful typing of this report.

The block diagram shown in Fig. 2.13 was designed at the Xebec Computer-Aided Design Center at UNR. The CDC-CYBER 73Ø computer system, operated by the computer center of the University of Nevada system, was used in the study.

Parts of this report are based on a master of science thesis by J.D. Hart directed by M. Saiidi.

TABLE OF CONTENTS

LIST OF TABLES

LIST OF FIGURES

CHAPTER 1

INTRODUCTION

1.1 Introduction

The current trend toward incorporating the nonlinear effects in design of structures under extreme loads in seismic codes has raised interest in developing a better understanding of the nonlinear response of structural systems. In the case of earthquake loading, the underlying design philosophy is allowance for damage (cracking of concrete, yielding of steel, etc.) which may lead to significant nonlinearity in response. To determine whether the structure is capable of developing large deformations without collapsing, a nonlinear analysis is necessary.

Several analytical models for building structures have been developed and used to evaluate the seismic response under severe earthquakes. Because of major differences between bridge structures and buildings, these models generally cannot be used for bridges. Only a small number of investigators have studied the nonlinear behavior of bridge structures for earthquake loadings. This report presents a relatively simple nonlinear analytical model for lateral load analysis of highway bridges.

1.2 Object and Scope

Many factors are involved in earthquake modeling of bridges. In terms of the earthquake loading, the ground motion may include six components (three translations and three rotations), and these components can be different from one support to another. In terms of

modeling of bridge components, the idealization of superstructures and substructures as well as the boundary elements is an important factor that can influence the response considerably. The object of the study presented in this report was to develop an analytical model for nonlinear static and dynamic response of short highway bridges subjected to horizontal loads or ground motions perpendicular to the longitudinal axis of the bridge. The study was limited to short highway bridges with single column reinforced concrete piers and no intermediate expansion joints. The nonlinear effects at the foundations, pier bases, and the abutments were taken into account. The model was developed in conjunction with experimental testing of a highway bridge (Rose Creek Interchange) which was subjected to static loads and free vibration and exhibited a limited degree of nonlinearity in its response [11]. The measured response of the bridge was used to evaluate some of the features of the analytical model. The model was used to study the effect of the new bridge seismic design guidelines prepared by the Applied Technology Council [4] on the performance of the Rose Creek Interchange. In addition, the model was used to study the response of this bridge for several earthquake records with different peak ground accelerations.

1.3 Review of Previous Research

The amount of available research results on nonlinear seismic modeling of highway bridges is limited. An overall review of the published reports and articles on this subject shows that it was the 1971 San Fernando earthquake and the damage it caused on highway bridges which raised the interest of researchers active in seismic studies of bridges.

Several factors influence the nonlinear modeling of the earthquake response in bridges. Most of these factors have been studied in connection with building structures, but the results of the studies may also be applicable to bridges. Nonetheless, there are some parameters which are unique to highway bridges and need special treatment.

In short highway bridges, the lateral behavior is affected by the abutments, the foundation [12], and the substructures and superstructures. The following sections include a review of the previous research results on these components in addition to a review of the overall nonlinear bridge modeling for lateral loads.

(a) Reinforced Concrete Piers - Bridge piers may consist of one or more columns. Where more than one column is used, the columns in combination with pier caps form a frame which is likely to behave similar to building frames under horizontal loads. In multicolumn piers, pier cap to column connections and column bases are the critical regions and are likely to yield. In single column piers, the critical section is generally near or at the base. The bridges considered in the present study were limited to those with single column piers; and hence, the following review is focused on the post-yielding behavior of isolated reinforced concrete columns.

Takeda et al. tested a series of small scale columns subjected to static and dynamic loads and developed a hysteresis model which closely agreed with experimental results [42]. The columns were reinforced with a large number of ties to avoid shear failure. Common details were used to anchor the longitudinal bars in the footings. It was observed that the slippage of the steel in addition to deformations due to flexure and cracking of the column contributed to the top deflection of the columns.

The cyclic response of the columns was accompanied by stiffness degradation, the extent of which was a function of the previous deformation history.

Priestly and Park [35] reviewed the test results from several static and dynamic loadings of one-sixth to one-fifth scale bridge pier models. They noted that columns with adequate confinement were able to develop displacement ductilities of about six without failure. The concrete strain in those columns was as high as 5 percent. Experimental data also showed that, in tied columns where ties are designed based on the minimum ACI Code limit [3], failure is accompanied by the buckling of longitudinal bars. The hysteresis loops for spiral columns were found to be more stable and exhibited a larger amount of energy dissipation per cycle.

Many hysteresis models have been developed to simulate the cyclic behavior of reinforced concrete elements. The Takeda model [42] was designed to closely predict the response of several test specimens subjected to static and dynamic loads. The specimens described in Ref. 42 were of pier type with constant axial force; and, hence, the Takeda model may be considered appropriate for single column piers. However, the model has the disadvantage of being relatively complicated. Simpler models have been developed and compared with the Takeda model [39-41]. The studies on these models have shown that a simple model, called Q-Hyst, is able to produce results which are very close to those of the Takeda model. This model accounts for stiffness degradation of concrete under cyclic loads. Another hysteresis model which has been used in nonlinear seismic analysis of bridges is the bilinear model [5,21]. The bilinear model does not include the stiffness degradation effects, but

it is simple and has been used extensively for building structures.

(b) Foundation Elements - Recent studies by Douglas and Norris, Douglas and Reid, and Saiidi and Hart have confirmed that the foundation flexibility can significantly alter the static and dynamic response of bridges [12, 29, 38]. While the cyclic behavior of isolated footings and stiff single piles may be dominated by soil properties, the behavior of foundations supported on pile groups is affected by the interaction between the piles and soil making the modeling of grouped pile foundations complicated. Experimental results [1, 7, 34] on small scale single piles and pile groups have indicated that (a) the stiffness of pile foundations is amplitude dependent and decreases significantly as the displacement amplitude increases and (b) the average stiffness decreases as the number of cycles of loading increases.

Several methods have been developed to predict the lateral response of piles and pile groups ranging from beam (representing the piles) on elastic foundation [7] to subgrade reaction theory [33]. Another approach has been to treat the pile as a multielement structure with dampers, gap elements, and friction elements attached to each component [26]. With these models, it is possible to construct the force-displacement relationship for piles and pile groups. The process is relatively complex. Norris adopted the Ramberg-Osgood hysteresis model [36] to determine the rotational cyclic behavior of pile groups [29].

(c) Abutments - The 1971 San Fernando earthquake showed that bridge abutments are susceptible to ground motions [14, 32]. The backfill soil in many bridge abutments settled as a result of this earthquake.

Although abutments are important parts of bridges, their overall

response to earthquakes has not been studied in any detail. Chen and Penzien used finite element to idealize the abutment structure and the backfill [5]. Because of the complex nature of abutment structures and their interaction with soil, it appears that the entire abutment system should be represented by a combination of spring and line elements. In bridges where the superstructures and substructures are considerably "softer" than the abutments, the abutments have been assumed to be fixed [17].

(d) Elastomeric Bearing Pads - Bearing pads are used for thermal isolation of bridge decks from abutments by allowing for expansion of the deck. Neoprene pads have been commonly used in the United States for this purpose. To model the nonlinear effects produced by the pads, the initial stiffness and variations in the force-deformation characteristics of bearing pads need to be known.

Only a limited number of studies have concentrated on the cyclic testing of elastomeric bearing pads. Nachtrab and Davidson [27] studied the behavior of bearing pads under simultaneous compression and shear loads. Imbsen and Schamber [23] investigated the stiffness and energy absorption characteristics of bearing pads subjected to dynamic loading at various load rates and amplitudes. The results of these studies indicate the following trends: a) cyclic shear stress vs. strain curves exhibited a softening effect even at low amplitudes; b) once a pad was deformed in shear, a residual shear force at zero deformation was present; c) residual shear strains increased as the maximum strain increased; and d) higher strain rates resulted in larger stiffnesses. No extensive studies on the hysteresis modeling of bearing pads can be found in the available literature.

(e) Nonlinear Modeling of Highway Bridges - Many analytical models have been developed for inelastic seismic analysis of building structures subjected to earthquake loads. These models, however, are not generally appropriate for bridge structures because of the considerable differences between bridge and building systems. Only a small number of nonlinear analytical models have been developed specifically for seismic analysis of bridges. Chen and Penzien [5] developed a finite element model for highway bridges utilizing an elasto-plastic model to represent the nonlinear effects. The model was used to analyze a three-span reinforced concrete box girder bridge subjected to earthquake motions. Extensive parametric studies were performed to determine the sensitivity of the model to various modeling parameters. In a study by Gillies and Shepherd [17], a two-span highway bridge was analyzed assuming that the elastomeric bearing pads remained elastic and the foundations were fixed. These assumptions restricted the nonlinear response to the substructure and superstructure. In this study, the differences in responses predicted using a three-dimensional model rather than a planar frame model and the effect of torsional vibrations were also studied.

Duxin developed an analytical model for railroad bridges with simply supported girders [13]. A finite element model was used to represent the linear and nonlinear behavior of soil. It was found that the nonlinear effects produced by the behavior of soil significantly altered the response at the foundation and the structure.

More recently, a computer code, called "NEABS," was developed by Penzien and Tseng and was later modified by Kawashima, Imbsen, Nutt, Liu, and Chen. The users' manual for the latest version of this program is presented in Ref. 22. The analytical model implemented in NEABS

allows for nonlinear three-dimensional boundary elements in addition to linear and nonlinear intermediate expansion joint elements capable of accounting for the effect of energy absorbing components. Both straight and curved girders are allowed. A yield surface is defined for biaxial response of pier columns.

CHAPTER 2

ANALYTICAL MODELING

2.1 Introduction

This chapter describes the development of an analytical model for static and dynamic analysis of highway bridges subjected to lateral loading. The underlying general assumptions and idealization are explained, and the limitations on the application of the model are presented. A new hysteresis model to simulate the cyclic behavior of some of the bridge components and the experimental data supporting the model are discussed. Finally, the analytical capabilities of the model and the related assumptions are presented.

2.2 Structural Modeling Method

The analytical model was developed to compute bridge response for horizontal loads applied in the transverse direction. The loads may be external static forces, inertial forces due to free vibration caused by an initial displacement, or dynamic forces due to ground motions. The modeling technique, for most parts, followed the available procedures which have proven to be appropriate for dynamic modeling of structural systems. For parts where no established procedure could be found, new methods were developed and judgment along with experimental data was used. Every attempt was made to avoid unnecessary complexities in the model.

(a) Assumptions and Idealizations - Figure 2.1 shows a schematic view of one-half of a five-span bridge model. The structure was assumed to consist of a series of massless line elements, translational springs, and rotational springs. The bridge structure was assumed to be either

fully or approximately symmetric, with "approximate symmetry" defined as having no drastic difference between the stiffness and geometric properties of components located at positions which are symmetric with respect to the center of the bridge. This assumption made it possible to restrain many of the possible degrees of freedom (DOF's) as explained below.

(i) Degrees of Freedom: Out of the possible six DOF's in a space frame, only three were allowed for the nodes on the deck and two at pier bases (Fig. 2.2). The deck nodes were allowed to displace in the transverse direction (X axis), rotate about the vertical axis (Z), and rotate about the longitudinal direction of the bridge (Y axis). The vertical displacement was restrained because no significant axial shortening of the piers and no settlement of the footings and abutments were expected. The deck vertical displacement at the abutment bearings was also restrained because the vertical displacement of the bearing system was expected to have taken place as a result of dead load before lateral loading of the bridge. In bridge structures with monolithic abutments, the assumption of no vertical displacement is even more appropriate if no abutment settlement is expected. The displacements along the length of the bridge (Y direction) deck were also assumed to be negligible due to the expected insignificant axial deformation of the deck and symmetry of the bridge. Rotation about the X axis was restrained at all points because lateral loading of the bridge would not produce such rotation. In addition to the restrained DOF's explained above, rotation about the Z axis was assumed negligible at pier bases. This was believed to be a reasonable assumption because of the relatively large torsional stiffness of footings and, particularly, pile

foundations.

(ii) Nodal Points: Structural nodes were assumed to be located at the intersection of pier and deck elements. In addition, one node was assumed at each pier base and each abutment. No intermediate nodes were assigned on the deck elements. This assumption has been used in girders and columns of building frames and has been found to be sufficient for an accurate representation of the structure. In bridge structures, of course, span lengths are relatively large and intermediate deck nodel points may seem necessary. However, as it is demonstrated in chapter five of this report and chapter five of Ref. 18, absence of intermediate nodes did not lead to any pronounced inaccuracies in calculation of the free-vibration and earthquake response of bridges.

(iii) Loads: Only horizontal loads in the X direction were applied at nodal points (Fig. 2.1). The loads may be static, or dynamic produced by inertial forces of bridge masses due to either free vibrations or ground motions. Bridge masses were assumed to be lumped at the nodal points. Tributary masses were used. For pier base nodes, it was assumed that the portion of the soil with a depth ten times the pile diameter will move with the node.

(iv) Geometric Nonlinearity and Gravity Effects: Deformations of the structure were assumed to be sufficiently small to allow for the undeformed configuration of the structure to prevail.

The gravity effects were included in the model by making appropriate reduction in the structural stiffness matrix. A procedure to take into account the gravity effects is presented in Ref. 30.

(b) Structural Components -

(i) Deck Elements: The deck system was assumed to be continuous with

no intermediate expansion joints. Deck elements were idealized as prismatic line members (Fig. 2.1) which remained elastic in the analysis. The latter assumption is valid because, to satisfy the strength and serviceability requirements for dead and live loads, bridge decks usually have large rigidity and strength against lateral bending.

Figure 2.3 shows the unrestrained DOF's on a deck element. Allowing for shear deformations, the stiffness matrix for this element is

$$[K]_d = \begin{bmatrix} \frac{12R}{L^2} & \frac{6R}{L} & -\frac{12R}{L^2} & \frac{6R}{L} & \emptyset & \emptyset \\ & 4R + \gamma R & -\frac{6R}{L} & 2R - \gamma R & \emptyset & \emptyset \\ & & \frac{12R}{L^2} & -\frac{6R}{L} & \emptyset & \emptyset \\ & & & 4R + \gamma R & \emptyset & \emptyset \\ & \text{Symm.} & & & \frac{GJ}{L} & -\frac{GJ}{L} \\ & & & & & \frac{GJ}{L} \end{bmatrix} \quad (2.1)$$

In which

$\gamma = 4\beta$;

$\beta = 3EI/GAL^2$;

A = effective shear area;

E = modulus of elasticity of concrete;

G = shear modulus;

I = moment of inertia about the centroidal axis in the Z direction;

J = torsional inertia;

L = element length;

$R = EI/L\ (1 + 4\beta)$.

(ii) Pier Elements: Only single-column piers were considered in the analytical model. A pier element was assumed to consist of an infinitely rigid top part, an elastic line element, and a nonlinear rotational spring at the base (Fig. 2.4.b). The infinitely rigid end segment represents the segment from the centroid of the deck (where a node is defined) to the bottom of the deck. The rigidity for this segment is assumed to be infinity to account for the fact that pier cap sections are considerably wider than pier columns. This may not be the case for very wide columns, in which case the length of the rigid end block may be assumed to be zero.

The moment diagram for the pier is shown in Fig. 2.4 (c). The maximum moment ordinarily occurs at the base limiting the possibility of yielding only to the bottom. For prismatic columns, experimental studies have shown that the length of the yielded region of the column is approximately one-half of the column depth [16]. Many pier columns are weakened at the base to reduce or eliminate transfer of moments in one or two orthogonal directions. For these columns, the length of the yielded region may be assumed to be equal to the length of the "weak" part. In idealizing pier elements, the inelastic deformations (deformations beyond cracking of concrete) are accounted for by a nonlinear rotational spring concentrated at the base (Fig. 2.4.b).

The deformed shape of a pier element, excluding relative displace-

ment of end nodes, is shown in Fig. 2.5. The moment-rotation relationship for the elastic part and the rotational spring can be written as:

$$\begin{Bmatrix} M'_A \\ M_B \end{Bmatrix} = [K'] \begin{Bmatrix} \theta'_A \\ \theta_B \end{Bmatrix} \qquad (2.2)$$

in which

$$[K'] = \frac{1}{\frac{1}{12}\left(\frac{L}{EI}\right)^2 + f_B \frac{L}{3EI} + S\left(\frac{L}{EI} + f_B\right)} \times \begin{bmatrix} \frac{L}{3EI} + f_B + S & \frac{L}{6EI} - S \\ \text{Symm.} & \frac{L}{3EI} + S \end{bmatrix}$$

In which

f_B = flexibility of the rotational spring;

$S = 1/GAL$

The stiffness matrix, including the effect of the rigid end, is determined by transforming M'_A to M_A as shown in Fig. 2.6. The moment equilibrium of the rigid end segment leads to:

$$M_A = (1 + \lambda_A)M'_A + \lambda_A M_B$$

For the total element, the equilibrium equation can be written as:

$$\begin{Bmatrix} M_A \\ M_B \end{Bmatrix} = \underbrace{\begin{bmatrix} 1 + \lambda_A & \lambda_A \\ \emptyset & 1 \end{bmatrix}}_{[E]} \begin{Bmatrix} M'_A \\ M_B \end{Bmatrix} \qquad (2.3)$$

The stiffness matrix for the element shown in Fig. 2.5 is determined from:

$$[K] = [E]^T [K'] [E] \tag{2.4}$$

This matrix does not include the effect of torsion and relative lateral displacements associated with the possible DOF's for pier elements (Fig. 2.7). Because torsion terms in the stiffness matrix are uncoupled from other terms, they can be added after the effect of other deformations are included. The relationship between end rotations of the pier and lateral displacements is:

$$\begin{Bmatrix} \theta_A \\ \theta_B \end{Bmatrix} = [T] \begin{Bmatrix} \delta_A \\ \phi_A \\ \delta_B \\ \phi_B \end{Bmatrix} \tag{2.5}$$

in which

$$[T] = \begin{bmatrix} -\frac{1}{L} & 1 & \frac{1}{L} & 0 \\ -\frac{1}{L} & 0 & \frac{1}{L} & 1 \end{bmatrix}$$

Other parameters are shown in Fig. 2.8. The complete stiffness matrix for the pier element is obtained from:

$$[K]_p = \begin{bmatrix} [T]^T[K][T] & \begin{matrix} 0 \\ \hline \frac{}{GJ} \\ \hline \frac{}{L} \end{matrix} \\ 0 & \end{bmatrix} \tag{2.6}$$

The moment-rotation relationship for the piers was developed primarily for single-column piers weakened near the base. The cracking of concrete and yielding of steel were assumed to be limited to the weak

deformations of the foundation play a major role in the response of bridge structures subjected to lateral loads [11, 13]. The complicated nature of pile-soil interaction in pile foundations makes it particularly difficult to accurately model the response of the pile group without implementing complicated analytical procedures. Based on the state-of-the-knowledge in this area, perhaps the most justifiable means of dealing with pile foundation behavior is through the use of a simplified, approximate approach. This approach should focus on the trends detected in pile group behavior and should reflect the soil properties and the geometry of the foundation.

The idealization of the foundation in the model is shown in Fig. 2.9. The effective mass of the foundation is restrained by a translational and a rotational spring. It is known that the force-deformation properties of pile foundations generally result in a curved relationship. This curve can be calculated based on the soil profile, the pile diameter, and the pile spacing. The calculation process, which is relatively complicated, is discussed in Ref. 29.

(iv) Elastomeric Bearing Pads: The bearing pad idealization used in the analytical model is shown in Fig. 2.10. The abutment point mass, which consists of one-half of the mass of the exterior span, is restrained by one translational and two rotational springs.

Experiments have shown that the vertical stiffness of bridge bearing pads is relatively large due to the reinforcing laminations which reduce the lateral bulging of individual layers. The force-deformation curves for vertical response also exhibit some stiffening effects due to the compaction of neoprene layers as loading increases. Considering the unrestrained DOF's explained above, the vertical stiffness of the

section. The model may be used for approximate modeling of fully prismatic columns by assuming an appropriate length for the plastic hinge. A plastic hinge length equal to one-half of the section effective depth has been used by some researchers [16, 31].

Rotation is defined as the ratio of top deflection at a cantilever column over the length of the column excluding the rigid segment. It was assumed that the column outside the weak region will remain elastic. It was further assumed that the shear stiffness of different segments is independent of load/deformation amplitude and is equal to the elastic shear stiffness. The rotation for cracking, yielding, and a moment beyond yielding can be determined from Eqs. 2.7-2.9. In developing these equations, it was assumed that L_p is considerably smaller than L. The third term in each of the equations is due to shear.

$$\theta_c = (M_c/E)(L_p/I_1 + L/3I_2) + M_c/GAL \qquad (2.7)$$

$$\theta_y = \phi_y L_p + M_y L/3EI_2 + M_y/GAL \qquad (2.8)$$

$$\theta_u = \phi_u L_p + M_u L/3EI_2 + M_u/GAL \qquad (2.9)$$

in which

θ_c, θ_y, θ_u = rotation at cracking, yield, and ultimate (defined as any point beyond yielding), respectively;

ϕ_y, ϕ_u = yield and ultimate curvatures, respectively;

I_1 = gross moment of inertia for the weak section;

I_2 = gross moment of inertia elsewhere;

M_c, M_y, M_u = cracking, yield, and ultimate moments at the weak section, respectively.

(iii) Foundations: It is known that the translational and rotational

bearing pads enters the analysis only in modeling the rotation of the abutments about the longitudinal axis of the bridge. Due to the relatively high vertical deck forces acting on the pads, variations in the vertical force due to deck rotation are not expected to produce any significant nonlinear effects. Therefore, the abutment springs restraining rotation about the longitudinal axis of the bridge were assumed to be linear.

(c) Hysteresis Models - The force-deformation relationships for nonlinear springs subjected to cyclic loads are controlled by hysteresis models. Two hysteresis models were used in the analytical model: the trilinear Q-Hyst model (TQ-Hyst) and the Ramberg-Osgood model [36]. These models were chosen because they exhibit the general nonlinear characteristics of the elements they are representing.

(i) The TQ-Hyst Model: TQ-Hyst is a modified version of a previously developed hysteresis model, Q-Hyst [39, 40]. The Q-Hyst model operates on a bilinear primary curve (defined as the force-deformation relationship for the first quadrant of the first loading cycle). The break point on the primary curve corresponds to the force or deformation at which there is a significant reduction in the stiffness. For reinforced concrete elements, this point usually corresponds to the yielding of steel. The primary curve for uncracked reinforced concrete members ordinarily includes another break point which corresponds to the cracking of concrete. This point, however, is ignored in the Q-Hyst model. While the exclusion of the cracking point may not lead to any significant inaccuracies in results for systems with moderate to large nonlinear deformations [40], it can result in underestimating the stiffness and energy absorption of members subjected to relatively

small-amplitude displacements or loads which correspond to the points between cracking and yield points. It appears, therefore, that a trilinear primary curve is more suitable for such cases. Another advantage of a trilinear primary curve over a bilinear one is that, if the measured relationship for an element is indeed curved and a piece-wise (consisting of straight segments) is to idealize the primary curve, a trilinear relationship can represent the primary curve closer than a bilinear one. A disadvantage associated with a model operating on a trilinear curve, of course, is that it is more complicated.

One measure of complexity of hysteresis models is the number of "rules" they include. A rule defines the stiffness for points on a specific part of the hysteresis curves and specifies what the following rules are going to be in the event a force/deformation increment results in passing a break point, crossing the deformation axis, or changing the load direction. The Q-Hyst model included four rules, while the TQ-Hyst model incorporates six (Fig. 2.11) as described below. Both models assume that the primary curve is anti-symmetric.

Definitions:

Loading: Increasing the absolute value of the force

Unloading: Decreasing the absolute value of the force in one direction

Load Reversal: Changing the force and its sign simultaneously

P = Any new point

K = Stiffness

F = Force

D = Deformation

Note: The rules of the TQ-Hyst model apply to both the negative and

positive force regions. In the negative force region, use absolute values of forces and change the labeling of break points to their "primed" counterparts.

U_m' is a point on the primary curve with the same absolute value of force/deformation as that of U_m.

Rule 1:

1.1 Loading:

if $F(P) \leq F(C)$ K = slope of OC; go to RULE 1

if $F(P) > F(C)$ K = slope of CY; go to RULE 2

1.2 Unloading and Load Reversal:

K = slope of OC; go to RULE 1

RULE 2

2.1 Loading:

if $F(P) \leq F(Y)$ K = slope of CY; go to RULE 2

if $F(P) > F(Y)$ K = slope of YU; go to RULE 4

2.2 Unloading (unloading point R):

K = slope of RC'; go to RULE 3

RULE 3

3.1 Loading:

if $F(P) \leq F(R)$ K = slope of RC'; go to RULE 3

if $F(P) > F(R)$ K = slope of CY; go to RULE 2

3.2 Unloading:

K = slope of RC'; go to RULE 3

3.3 Load Reversal:

if $F(P) \leq F(C')$ K = slope of RC'; go to RULE 3

if $|F(P)| > |F(C')|$ K = slope of C'Y'; go to RULE 2

RULE 4

4.1 Loading:

K = slope of YU; go to RULE 4

4.2 Unloading:

S = (slope of C'Y)*$(D_{y/Dmax})^{0.5}$

K = S; go to RULE 5

RULE 5

5.1 Loading:

5.1.1 if last unloading point on YU; go to 5.1.2

if $F(P) \leq F(R')$ K = S; go to RULE 5

if $F(P) > F(R')$ K = slope of $X_oU'_m$; go to RULE 6

5.1.2

if $F(P) \leq F(U_m)$ K = S; go to RULE 5

if $F(P) > F(U_m)$ K = slope of YU; go to RULE 4

5.2 Unloading:

K = S; go to RULE 5

5.3 Load Reversal:

K = slope of $X_oU'_m$; go to RULE 6

RULE 6

6.1 Loading:

if $F(P) \leq F(U'_m)$ K = slope of $X_oU'_m$; go to RULE 6

if $F(P) > F(U'_m)$ K = slope of Y'U'; go to RULE 4

6.2 Unloading (unloading point R')

K = S; go to RULE 5

A study of the available test data for cyclic response of reinforced concrete piers [16, 35] and pile foundations [7, 26, 33, 34], showed that the TQ-Hyst model can reasonably represent the overall cyclic

behavior of these elements, and hence, the model was used to idealize the nonlinear springs to simulate these components. Due to the scarcity of experimental data for cyclic, lateral and rotational response of footing foundations and pile foundations, a qualitative representation of the behavior of these components by TQ-Hyst was considered adequate. Refinements in the model may be warranted as more experimental data become available.

(ii) The Ramberg-Osgood Model: The Ramberg-Osgood hysteresis model was originally developed to model the nonlinear behavior of steel connections [36]. A qualitative study of the experimental data from tests performed on elastomeric bearing pads indicated that the Ramberg-Osgood model can reasonably represent the hysteretic behavior of these pads [23, 27].

The primary curve for the Ramberg-Osgood model is shown in Fig. 2.12. The two rules of the model are outlined as follows:

1. Loading on Primary Curve:

$$D = F(D_y/F_y)(1 + |F/F_y|^{(G-1)}) \qquad (2.10)$$

2. Unloading and Load Reversal:

$$D = (F-F_o)(D_y/F_y)(1 + |(F-F_o)/2*F_y|^{(G-1)}) + D_o \qquad (2.11)$$

where:

F = force at an arbitrary point;

D = deformation at an arbitrary point;

F_y = force at point A;

D_y = deformation at point A;

F_o = force at largest excursion point;

D_o = deformation at largest excursion point;

G = nonlinearity parameter.

Given information about the initial stiffness and the nonlinear character of an element idealized by the Ramberg-Osgood model, the primary curve of the element can be defined by specifying only three parameters: F_y, D_y, and G. The model is very versatile. Figure 2.12 shows the range of nonlinearity that can be obtained by varying the nonlinearity parameter, "G". A "G" value of one will produce a linear primary curve, while a "G" value of infinity will produce an elasto-plastic primary curve.

2.3 Static and Dynamic Analysis Procedures

The analytical model was developed to carry out the following analyses:

1) Static analysis for lateral loads
2) Free-vibration analysis
3) Earthquake response history analysis.

In addition, the model may be used to determine frequencies and natural mode shapes of the bridge based on initial or instantaneous stiffness. Figure 2.13 shows a flow diagram for the model.

Several steps were taken to reduce the amount of computation and computer memory space: 1) Full advantage was taken of the symmetry of the element stiffness matrices in storing the stiffnesses; 2) Nodes and DOF's were numbered in a manner that would minimize the bandwidth of the structural stiffness matrix (Fig. 2.14); 3) Stiffness submatrices corresponding to lateral and rotational DOF's were partitioned and static condensation was used to reduce the size of the matrix to be inverted; 4) The condensed structural stiffness was stored as a lower triangular matrix for inversion. Five subroutines from the International Mathematical and Statistical Library [25] were used in the

model. Subroutine LINP1B was used to invert the submatrices in the static condensation portion of the program. Subroutine LEQ1S was used to invert the structural stiffness matrix and subroutines EQZQF, EQZTF, and EQZVF were used to perform the eigenvalue analysis.

(a) Static Analysis - The model can analyze the bridge for static lateral loads applied at nodes (Fig. 2.1). The load increments can have an arbitrary distribution, and can have different signs; thus allowing for cyclic loading of the bridge. In the end of analysis for each load, the status of the nonlinear elements is checked and their stiffnesses are updated as necessary. To insure that the primary curves of the elements are followed closely, the loads should be applied in small increments. The model calculates displacements, rotations, ductilities (defined as the ratios of maximum rotation and yield rotation), and internal forces for each load increment.

(b) Free-Vibration Analysis - The model can be used to determine the free-vibration response of a bridge system subjected to initial displacements caused by specified static loads. This feature in the model was specifically developed to analyze the Rose Creek Bridge which was subjected to static loads, then the loads were suddenly released producing a free-vibration response. For the free-vibration analysis part of the model, it is not possible to specify an initial displacement. Rather, the static loads causing the initial displacement need to be provided. The initial stiffness matrix and the status of the hysteresis curves for different elements are those determined at the end of the last static load increment. The damping of the system is assumed to be proportional to both the mass and the instantaneous stiffness.

This type of damping is referred to as Rayleigh damping [6] and has been commonly used in models for building analysis [30, 39].

The differential equation of motion is formulated in an incremental form and integrated at small time intervals using Newmark's β method [28]. The time interval used for numerical integration is typically taken as approximately one-tenth to one-twentieth of the shortest period of the system to insure convergence. A β value of 0.25, which corresponds to constant acceleration over each time interval, is used in the model. This procedure results in an unconditionally stable response for elastic systems. The accelerations and lateral displacements for specified DOF's are calculated for each time interval and stored for plotting the response histories.

Because the mass and stiffness coefficients used to create the Rayleigh damping matrix are functions of the frequencies for the first two vibration modes of the system and because convergence limits depend on the shortest period of the system, an estimate of the frequencies of the model would be needed for dynamic analyses.

(c) Earthquake Response History Analysis - The analytical model can be used to determine displacement and acceleration histories for an input ground motion record. The motion is assumed to be the same at all foundations and abutments. This assumption ignores the possibility of having different ground motions at different supports due to (a) the time delay for the earthquake wave to travel from one support to the other, or (b) different geotechnical/foundation characteristics, or both of these. For relatively short bridges, however, the difference in ground motions may be assumed negligible because the travel time for the earthquake wave may be short and because, over a relatively short

distance, variation in geotechnical properties may be small. The fact that the large differences between the geometry of abutment systems and pier foundations may introduce significant differences in the input motion even for short bridges still remains true. However, this possibility is ignored to keep the model simple.

Many of the techniques used in free-vibration analysis are also applied for earthquake response analysis. The differential equation of motion is written in incremental form and integrated using Newmark's method [28]. Because the equation of motion is integrated using very small time increments to insure convergence and stability, updating the stiffness and Rayleigh damping matrices after each cycle would be a costly and inefficient process. Furthermore, changes in these matrices over a very small increment of time are assumed to be negligible. Therefore, the stiffness and damping matrices are updated only at a specified number of time increments. Judgment and experience indicate that the stiffness and damping matrices need to be updated approximately one hundred times each second.

CHAPTER 3

THE TEST STRUCTURE

3.1 Introduction

This chapter describes the Rose Creek Interchange, the procedure used in its seismic design, and the static and dynamic experimental tests that were performed on the bridge in May 1982. Steel reinforcement details, in addition to the material properties, are also presented. The section on the experimental testing of the bridge discusses only those tests which were simulated in the analytical studies presented in this report.

3.2 The Rose Creek Interchange

The Rose Creek bridge is a five-span reinforced concrete multicell box girder bridge with a total length of 400 ft., located on highway I-80 near Winnemucca, Nevada (Fig. 3.1). The substructure consists of four single piers (Fig. 3.2) and the abutments, all of which are supported on pile foundations. The deck is continuous with no intermediate expansion joints and has monolithic connections to the piers. Each end of the deck is supported by 5 neoprene elastomeric bearing pads with a thickness of 3 in. and planview dimensions of 10 X 14 in. such that the 14 in. edge is in the transverse direction. The drawings call for 0.25 in. embedment of the pad thickness in the deck and the abutment. The specified durometer rating for the pads was 50, and the actual value at the time of shipment was 52. Grade 60 steel and concrete with a 28-day compressive strength of 3000 psi had been specified. The measured yield stress for #11 bars (the only bars likely to yield for lateral loading) was 63.3 ksi based on 3 samples. The

measured concrete compressive strength in 28 days was 4445 psi based on 8 samples for piers 1 and 3 and 3550 psi based on 51 samples for the deck.

The reinforcement distribution in the piers is shown in Fig. 3.3. The connection to the footing is a hinged connection in the longitudinal direction of the bridge, but is moment resistant in the transverse direction. The dowels are made from #11 bars in all the piers. Because no yielding of the reinforcement in the deck was expected, the deck steel did not enter the analysis and is not shown.

3.3 Seismic Design Procedure

The bridge was designed based on the 1965 AASHO document [2], Standard Specifications for Highway Bridges, the Interim Specifications through 1967, and the 1966 BPR Ultimate Strength Design Criteria. According to the 1965 AASHO Code, because the bridge was supported on pile foundations, the horizontal earthquake force was 6 percent of the dead load and was treated as a service load. No provisions to account for the effect of foundation flexibility were included. In the design process, the foundation was assumed to be rigid and the elastomeric bearing pads were treated as hinged supports. The design forces were determined using the so called "Lollipop Method" which was a common method at the time [24]. Based on this method, 6 percent of the dead load reaction for each pier was applied horizontally; and the shear and moment at the base of the pier were determined. Because the pier connection to the pile cap was moment resistant only in the transverse direction of the bridge, the computation was carried out only for this direction.

3.4 Experimental Studies

The Rose Creek Bridge was subjected to static and dynamic test loads [11]. The static loads were applied in the transverse direction of the bridge at the intersection of the piers and the deck by four hydraulic rams acting at an angle of 45o (Fig. 3.4). This method of loading was first introduced and used by Douglas [11]. The rams were loaded manually at a small rate. Temporary reaction foundations were built to support the rams. The bridge was loaded to several amplitudes, and the ram loads were simultaneously released to allow for free-vibration testing of the bridge. Of relevance to the study presented in this report were the static and free-vibration behavior of the bridge for the design loads and loads totalling approximately one and one-half times the design load.

The static data collected included the lateral deflection of the deck at the ends, the pier caps, and the center of the middle span. The deflections of the ends of the deck and at the centerline of the bridge deck were measured with dial gages. A temporary structure was erected at the center to serve as a fixed reference for the deflection measurement at the centerline of the bridge. The deck static deflection measurements at the pier caps were obtained by using a theodolite to observe a micrometer screw target which moved as the bridge deflected.

The footings were excavated to allow for close inspection of the pier to pile cap connections and to measure the dynamic response of the pile caps. Because the shear keys (Fig. 3.3) were the weakest part of the piers while they carried the maximum moment, they were examined very carefully to detect any crack formation or propagation.

The dynamic response of the structure, including its foundation

elements, was measured using a four channel system with four force balance accelerometers. The data were recorded on an FM tape recorder for later digitization and analysis. The dynamic data were measured by a "fixed" reference accelerometer and a triplet of "moving" accelerometers. Data were recorded at stations fifteen feet apart on the bridge deck. In addition, the motions of the bridge abutments were recorded along with the rotational and translational motions of the pier foundations.

Four load amplitudes were used in the study. Of importance to the static behavior of the bridges were two load levels, one at a total ram load of 320 kips (approximately the design load) and the other at 450 kips (approximately 1.5 times the design load). These loads were distributed equally among the four piers. The resulting static data and the response histories were recorded for analysis and digitization. The measured data along with the calculated results are presented in chapters 4 and 5.

CHAPTER 4

STATIC BEHAVIOR OF THE ROSE CREEK BRIDGE

4.1 Introduction

The Rose Creek Bridge was subjected to static loads as part of the experiments (Sec. 3.4). The analytical model described in chapter 2 was used to determine the response of the bridge under static test loads as well as a variety of other loads specified in seismic guidelines by AASHO [2] and ATC-6 [4]. This chapter presents the results of the analyses and a discussion about the effect of the assumptions made in the analytical model and seismic codes on the displacements and internal force distribution.

4.2 Response Under Test Loads

The static analysis feature of the model described in chapter 2 was used to calculate the response of the Rose Creek Interchange for test loads. The moment-curvature properties of the piers were determined using routine methods [31]. The concrete compressive strength used in calculations was 3550 psi, which was the average strength of fifty-one concrete samples taken during the construction of the bridge deck. Only eight samples had been taken from the concrete in piers, and they were for piers 1 and 3 with an average strength of 4445 psi. This could mean that the piers had a higher strength; but, because of the limited number of samples from piers and because concrete strength does not have a strong effect on component properties, the value for the deck was assumed to be representative of the concrete in the entire structure. The strain at the concrete compressive strength was assumed to be 0.002, and the ultimate strain was taken equal to 0.003. The Hognestad's

method [20] was used to define the shape of the stress-strain diagram for concrete with adjustments made in strain at the compressive strength and strain at crushing of concrete.

Only #11 bars (the dowels) were likely to yield. Three samples of #11 bars had been tested with an average yield stress of 63.3 ksi. However, because this stress was close to the specified value, the specified yield stress of 60 ksi was used with an assumed strain-hardening slope of 10 percent of the elastic slope, starting at the yield point. In computing the cracking moments of the piers, the modulus of rupture was found using the ACI [3] formula; and the effect of axial forces was taken into account. The moment-curvature values for pier bases are listed in Table 4.1. In this table, breakpoint 1 represents cracking. Breakpoint 2 is the effective yield point of the section and is determined by first plotting the moment-curvature diagram corresponding to the yielding of different layers of dowels and then idealizing the diagram by an equivalent trilinear curve. The third breakpoint is any point on the post-yielding branch of the idealized curve and is used in the model to determine the slope of the third branch. This point is not treated as the ultimate strength point. The section is assumed to have unlimited ductility.

For moments corresponding to each of the breakpoints, the bond slip rotations were computed assuming a uniform bond stress over the anchorage length [39]. The bond strength in these computations was taken from the 1963 ACI Code. The resulting bond slip rotations are listed in Table 4.1. The force-deformation characteristics of the pile foundations were determined based on the procedures outlined by Norris [29] and are listed in Table 4.1. Similar to piers, the third breakpoint is used only to determine the slope of the third branch and

is not used as an ultimate point. To determine the basic backbone curve for the abutment springs, the available guidelines prepared by the manufacturer were initially used, but the results led to unreasonably "soft" abutments. Estimates of the initial stiffness of the pads for ambient levels of vibration were available in a report by Gates and Smith [15]. These values were used as the initial slope of the Ramberg-Osgood primary curves (Table 4.1). A brief parametric study indicated that a "G" value of 1.5 in the Ramberg-Osgood function produced a good correlation between the calculated and measured free-vibration histories. The P-Δ effect was considered in all of the analyses.

Because the hydraulic rams used to load the bridge acted at a 45 degree angle, there were, in effect, a horizontal and a vertical component of load applied to the structure (Fig. 3.4). The vertical component of the load was eccentric with respect to the centroidal axis of the pier, thus producing an additional base moment. Because the model is capable of accepting only horizontal forces applied at the nodes, the additional base moment caused by the vertical component was transformed into an equivalent horizontal force acting at the deck centroid. An additional translation of forces was necessary to determine an equivalent horizontal force acting at the deck centroid (as opposed to the bottom of the deck where the actual loads were applied) while producing the same base moment as that caused by the horizontal ram loads. The structural loading configuration used in this analysis was the 56 ton per ram case, which was approximately 1.5 times the design lateral load for the bridge. This loading produced an equivalent horizontal load of 84.6 kips per pier which was applied in 20 equal increments in the analysis.

The calculated and measured static force-displacement curves for all of the deck nodes and the bridge centerline are shown in Fig. 4.1. The calculated internal forces indicated that none of the foundation and pier base springs passed the first breakpoint of their trilinear primary curves. The hysteretic behavior of these springs was controlled by the TQ-Hyst model. This confined the nonlinearity to the abutment springs, which are controlled by the Ramberg-Osgood model. The calculated deformations of the abutment springs were relatively small indicating that the entire system exhibited only a small degree of nonlinearity. This observation is reflected in the calculated loading curves for the deck in which only the abutment nodes and, to a lesser extent, the exterior piers exhibited a slight nonlinear effect. A plan view of the calculated and measured deflections at the maximum load is show in Fig. 4.2. All of the deflections are in very good agreement (with differences of 10 percent or less) except for pier 4 in which the calculated response is 30 percent greater than the measured value. Because the correlation is close for pier 1 (which is similar to pier 4), the poor correlation at pier 4 can perhaps be attributed to a measurement error. Excluding the response of pier 4, the results from the static analysis are in very good agreement with the measured response. However, it should be noted that, since only the abutments exhibited any nonlinear behavior, the nonlinear capabilities of the model could not be rigorously tested under these loading conditions.

4.3 Design Procedures for Earthquake Loads

To compare the seismic design forces recommended by the code which was in effect at the time of the design of the Rose Creek Interchange and to evaluate the overall performance of the bridge for code loads,

the bridge was subjected to several elastic and inelastic analyses. Two earthquake design codes were considered in the study. One was the code used in designing the bridge [2], and the other was the guidelines recommended by the Applied Technology Council [4]. The latter was recently adopted by the Federal Highway Administration as a design guideline and by AASHTO as a "guide" specification. The AASHO-65 method was described in Sec. 3.3. The ATC-6 guidelines are presented in the following paragraphs.

The ATC-6 method is probably one of the most comprehensive earthquake design codes for bridges. The basic philosophy used in this code is that (1) in the event of a small to moderate earthquake, structural components should remain elastic, and (2) large earthquakes should not lead to the collapse of the bridge.

Several factors are taken into account in determining the design loads. An acceleration coefficient is assigned depending on the geographical location of the bridge. A site coefficient is also included to account for the effect of geotechnical characteristics on the response. For bridges in regions with moderate to severe seismic activities (with an acceleration coefficient of Ø.29 and higher), an importance factor is assigned which depends on the impact that the potential loss of the bridge may have. The value of the acceleration coefficient is also used to find the "seismic performance category" which in turn is used to specify the analysis procedure and determine the design forces.

Two analysis procedures are outlined, both using an elastic spectral analysis. Procedure 1 is recommended for "regular" bridges (those with no abrupt change of mass, stiffness, or geometry along their

spans/supports) and utilizes a unimodal analysis. Procedure 2 is for "irregular" bridges (those violating the conditions of a "regular" bridge) and uses a multimodal analysis. Using any one of the procedures, the bridge is analyzed for each direction and the resulting internal forces are combined according to two specified load cases. The design loads used in the analysis are ultimate loads, but an elastic, as opposed to ultimate, analysis is used to determine the internal forces. To account for the nonlinear action of structural components, which prevents an unlimited build up of internal forces, a response modification factor is specified which is used to reduce the forces found from the analysis.

The effect of foundation flexibility is mentioned. For regular bridges, it is stated that boundary conditions at the abutments and piers can be accounted for in the modeling, while, for irregular bridges, an iterative method to determine an equivalent elastic stiffness for the abutments is outlined.

4.4 Response Under Code Loads

The Rose Creek Bridge was designed using the lollipop method [24] based on the 1965 AASHO Code [2]. Because the drawings had called for a 1/2 in. gap between the deck and the shear keys at the abutments, this gap was considered adequately small to treat the deck-to-abutment joint as a hinged connection. The actual gap, however, was approximately 3" wide, making the hinged assumption unjustified. The effect of the change in the gap width on internal forces is discussed in Ref. 37. In the following sections, the effect of analyzing the total structure as opposed to individual columns (used in the lollipop method) and the effect of using an inelastic analysis instead of an elastic analysis

recommended by ATC-6 are discussed. To study the latter effect, it was necessary to determine design forces based on the ATC-6 method. To be consistent with the original design assumptions, in all the cases presented in this section, the connections at the abutments were assumed to be hinged, and the pier foundations were assumed to be fixed.

(a) Lollipop Method vs. Analysis of Total Structure - As it was mentioned in the section on design procedures, the "lollipop method" was used in the design process assuming a horizontal force which was 6 percent of gravity. To determine how the internal forces would have been affected if an analysis of the total structure (as opposed to the individual pier analysis used in the lollipop method) had been carried out for the 6 percent of gravity load, an elastic analysis was performed. The resulting pier base moments and shears are shown in column "b" of Table 4.2. Note that, because of symmetry, only pier 1 and 2 forces are listed. It can be seen that the forces from the analysis of the total structure were slightly higher for pier 2 but lower for pier 1. The increase in the forces for pier 2 was seven percent while the decrease for pier 1 was 29 percent and smaller. The relatively large decrease in forces for pier 1 is due to the fact that, by applying the loads to the total structures, the abutments carry part of the loads applied at piers 1 and 4. The forces in piers 2 and 3 are only slightly affected by the abutments because these piers are relatively far from the ends. The minor increase in the forces for these piers is due to the slight bending of the deck caused by restraint against displacement at the abutments.

(b) Design Forces Based on ATC-6 - The ATC-6 guidelines were used to

determine the earthquake loads for the Rose Creek Bridge. The ground acceleration coefficient for the site of the bridge is 0.21 based on the ATC-6 isocurves shown in Fig. 4.3. The seismic performance category (SPC) was determined to be "C". Because the soil profile consists mostly of medium-stiff clay, a site coefficient of 1.5 was used. The response modification factor for moment is 3, which is used for single-column piers. A response modification factor of one is recommended for shear. As specified by ATC-6 for bridges with an SPC of "C", the moments should be increased by 30 percent for the design of the connections. The moments discussed in this report, however, are the pier moments and do not include the 30 percent increase. Because the bridge is "regular", the unimodal analysis (procedure 1) was used. The resulting parameters and their definitions are shown in Table 4.3. As it was mentioned in previous sections, in the ATC-6 guidelines, an elastic analysis of the bridge is used based on the ultimate loads; then a response modification factor is used to account for nonlinear effects. An inelastic static analysis appears to be more consistent with the loads, and would have been more desirable. However, perhaps due to the complexity of inelastic analysis and because of the fact that designers generally do not have access to inelastic analysis software, an elastic analysis is recommended. To determine the extent of approximation that the elastic analysis introduces in the results, a linear and a nonlinear analysis of the bridge for the loads recommended by ATC-6 were carried out using the analytical model explained in chapter 2. The force-displacement relationships are shown in Fig. 4.4. As expected, the line representing the elastic response was tangent to the initial part of the inelastic response curves. The initial part of

the inelastic response (for loads less than approximately 300 kips) represents the uncracked stiffness of the bridge. A substantial reduction of stiffness was observed as soon as the piers cracked. The exterior and interior piers cracked at approximately the same load. As a result, a relatively sharp breakpoint can be observed in the curves.

As was pointed out in previous sections, in the analytical model it is assumed that the shear strength of different members is sufficiently large to preclude any shear failure. Comparison of the maximum shear forces calculated from the nonlinear analyses with the ultimate shear strengths at the base of the piers determined using the ACI Code formulas [3] showed that the shear strength of pier 2 would have been exceeded by 30 percent and there would be a brittle failure.

No yielding of the piers occurred. The maximum ductility demand, with ductility defined as the ratio of maximum rotation to the yield rotation, was 0.6; and it occurred in the middle piers. The ductility ratio in piers 1 and 4 was 0.4. It was noted that the middle piers cracked before the others, forcing the deck ends to move in the opposite direction of the loads. This trend continued until piers 1 and 3 cracked. Another important observation was that, upon the cracking of the piers at the base, the moments at the pier tops increased significantly causing the reversal of shear at the bases of piers 1 and 4.

The maximum pier forces are listed in Table 4.4. It can be seen that the elastic analysis overestimated the moment for pier 2 by 43 percent and shear for this pier by 46 percent. The moment and shear for pier 1 were underestimated by 3 and 18 percent, respectively.

(c) Comparison of AASHO-65 and ATC-6 Forces - Table 4.5 shows the pier forces determined based on the loads specified by AASHO-65 using the

lollipop method and forces determined based on the ATC-6 procedure (with an elastic analysis). Because the forces from AASHO-65 were service loads while the ones from ATC-6 are ultimate, the AASHO-65 results were amplified by a load factor of 1.4 (the load factor used for seismic forces in the ACI Code [3]). It can be seen that shear forces based on the new code are as high as 7.5 times the forces from the old code. The differences in the moments are not as pronounced. The ratio of the moment based on the ATC-6 Code and that based on AASHO-65 is 1.5 for pier 1 and 2.7 for pier 2. The differences show that, if an identical bridge were to be designed using the ATC-6 guidelines, the "weak" parts at the base of the pier would have to be eliminated and additional steel reinforcement would be needed.

CHAPTER 5

FREE-VIBRATION RESPONSE

5.1 Introduction

The Rose Creek Bridge was subjected to free-vibration by the quick release of the ram loads. The main reasons for this part of the experiment were to determine the dynamic characteristics of the bridge [11] and to carry out system identification studies [10]. Although the measured response did not include any notable nonlinearity, the test data were used to evaluate, at least, some of the features and modeling methods used in the analytical model. This chapter presents the analytical and experimental results from free vibration of the bridge caused by the release of the largest test loads. A discussion about the correlation between the calculated and measured results is also presented.

5.2 Analytical and Experimental Results

The free-vibration response of the bridge was calculated using the analytical model described in chapter 2. The basic properties of bridge components were the same as those used for static nonlinear analysis (Sec. 4.2). The bridge was subjected to test loads which corresponded to an equivalent horizontal force of 84.6 kip per pier applied in 20 equal increments. Then the loads were released and the free-vibration response was found with initial conditions being those in the end of the last load increment. A damping ratio of 2 percent was used. In addition, it was assumed that the mass proportionality constant of the Rayliegh damping matrix was zero, thus filtering out the effects of the higher modes of vibration [6]. This is justified because the load

distribution was expected to excite only the lower symmetric modes and because higher modes are generally more vulnerable to small errors in measurement and computation. The time step used for numerical integration in the free-vibration analysis was 0.005 seconds, which is about one-fifteenth of the shortest initial period of vibration of the system. The choice for a value of G used in the idealization of the bearing pads (Sec. 2.2.c) seemed to be arbitrary due to the lack of experimental data. A brief sensitivity study showed that the effective period of the free-vibration response was sensitive to this value. It appeared that G = 1.5 resulted in a good correlation. It is suspected that a different value of G would have led to a good correlation if the tangent slopes of the primary curves were different from what was used.

The calculated and measured acceleration response histories are shown in Figs. 4.5 through 4.7. It can be seen that the analytical model predicted relatively large acceleration peaks at the abutments (Fig. 4.5) while, for pier top and pier bases, the calculated peaks were generally close to the measured values (Figs. 4.6 and 4.7). This can be an indication that the modeling of the abutment was not representative of the actual behavior. The fact that the calculated static displacements at the abutments were close to the measured values suggests that the primary curves for the abutment springs were reasonably accurate, and it is the assumed hysteretic behavior which may need some refinement. Such a task is not possible, however, due to inadequate experimental data on the cyclic behavior of elastomeric bearing pads.

The peak responses at the pier foundations were relatively small (Fig. 4.7). This was especially true for piers 2 and 3 where the soil profile consisted mainly of a relatively stiff clay. The correlation

between the calculated and the measured acceleration histories was relatively close during the first 3 seconds indicating a reasonable estimate of the foundation stiffnesses. It should be noted that none of the pier and foundation springs developed nonlinear deformations during the free-vibration response; and, hence, their hysteresis modeling could not be evaluated.

With respect to the free-vibration displacement histories (Figs. 4.5-4.7), it can be seen that a residual displacement was present in the abutment responses and, to a lesser extent, in the deck response at piers 1 and 4. A sensitivity study was carried out to determine whether the shift was due to the instability of the response caused by the time step used in numerical integration of the equation of motion. This possibility was thought to exist despite the fact that the time step had been adequately short to satisfy the stability requirements for elastic systems [28]. For inelastic systems, it is known that an unstable response may result even if the time step satisfies the stability requirements for elastic systems having the same periods of vibration. The sensitivity study showed that the residual displacements were not due to the choice of time step. The shift can be explained by observing the first few cycles of the displacement response. At the end of the first cycle, the maximum displacement occurs. From that point on, the displacement response dies out rapidly. Because of the nature of the Ramberg-Osgood model and because all of the subsequent cycles of displacement were smaller than the first cycle, a residual deformation of the same sign as that of the maximum deformation can be expected. Because the response of the exterior piers is strongly influenced by the abutment response, some shift can also be expected in the displacement

response of the deck and fcundation nodes of piers 1 and 4.

Despite the lack of complete agreement of the calculated and measured acceleration amplitudes and despite the slight lack of agreement in effective period in the latter part of the records, the calculated response was generally close to the measured response. However, because the degree of nonlinearity in both the measured and calculated responses was very limited, it can only be stated that the overall elastic modeling segment of the analytical model is reasonably representative of the physical system. The assumed hysteresis modeling methods remain to be tested until measured large-amplitude responses become available.

CHAPTER 6

RESPONSE HISTORY ANALYSIS

6.1 Introduction

The behavior of the Rose Creek Bridge subjected to different earthquake records with different peak accelerations is discussed in this chapter. Three earthquake records, each normalized to two different maximum accelerations, were used in the study resulting in a total of six earthquake analyses. The response of the bridge for these earthquakes is presented and the results for different earthquakes are compared. This chapter also reviews the safety of the bridge if an earthquake similar to those considered were to occur at the site.

6.2 Input Earthquakes

Three earthquake records were used to evaluate the seismic performance of the Rose Creek Bridge in the lateral direction. These were the corrected acceleration records obtained at El Centro NS 1940, Taft S69E 1952, and Castaic N21E 1971. These records were selected based on their overall frequency content and based on their response spectra characteristics in the period range covering the initial fundamental period of the Rose Creek Bridge.

The first 10 seconds of the acceleration records for the above earthquakes were used in the analysis (Fig. 6.1). It can be seen in Fig. 6.1 that the El Centro record has mainly low-frequency waves, while the Castaic record includes predominantly high-frequency waves. The frequency content of the acceleration record for Taft can be considered to be in between the El Centro and Castaic records.

The calculated initial fundamental period of the Rose Creek Bridge

was 0.4 sec. [18]. Because of the anticipated softening of the bridge components, the effective period is expected to increase. Shown in Fig. 6.2 are the response spectra for the above earthquakes. The different curves for each record correspond to the damping ratios of 0, 2, 5, 10, and 20 percent. The curves for each record have the same general trend. The following discussion, however, is more applicable to systems with a damping ratio of 5 percent and higher. To evaluate the expected effect of an earthquake, the pseudovelocity response may be used because it is a measure of earthquake energy. It can be seen that, for the El Centro record, as the system period increases from 0.4 sec., there is a substantial increase in velocity and the response remains relatively large for periods of up to 1 second. The El Centro response spectrum may, thus, be considered broad band and ascending (BBA) for the Rose Creek Bridge. For the Taft record, the response is somewhat insensitive to the period elongations of beyond 0.4 sec. and up to 2 seconds. This earthquake may be considered as having a broad band (BB) spectrum. Finally, the Castaic response spectrum may be considered to be narrow band (NB) as period elongation of beyond 1 sec. results in considerable reduction in the response. The above method of categorizing earthquake response spectra has been used by Derecho et al. [8] and Hodson [19].

Each earthquake record was normalized to two values of peak ground accelerations (PGA): (1) 0.1g to compare the resulting internal forces and deflections with the calculated and measured results from the static analysis for the ram loads (which were approximately equal to 0.1g), and (2) the maximum ground acceleration which was measured during the actual earthquake to evaluate the performance of the bridge for the actual base motion records.

6.3 Evaluation of the Response and the Behavior of the Bridge

The Rose Creek Bridge was analyzed for the records discussed in section 6.2 assuming a 5 percent damping for the first two elastic modes. A time step of 0.005 sec., which was approximately one-fifteenth of the shortest initial period of the bridge, was used to integrate the differential equation of motion. The stiffness matrix was updated once every 0.01 seconds. All the analyses included the P-Δ effect. The stiffness properties of the foundations for piers 3 and 4 were taken to be the same as those of piers 2 and 1, respectively, even though the soil profiles had some minor differences. This resulted in a symmetric response for the bridge.

(a) Response for Earthquakes with PGA of 0.1g - The response histories for different earthquakes normalized to a PGA of 0.1g are shown in Figs. 6.3-6.5, and the maximum absolute responses are listed in Tables 6.1 and 6.2. The maximum responses for static loads are also included in the tables to compare the static analysis results with those from the earthquake loads.

The response histories for different earthquakes have some common characteristics (Figs. 6.3-6.5). The acceleration responses at pier foundations for each motion are identical to the input acceleration indicating a relatively stiff foundation. Some amplification of the peak acceleration took place for El Centro in which the maximum absolute acceleration for pier base 1 was 0.16g and for pier base 2 was 0.14g. The Castaic record amplified the maximum acceleration to 0.15g and 0.12g for piers 1 and 2, respectively, while no significant amplification was evident for the Taft record responses.

Another common feature of the responses can be seen by comparing

the displacement histories of the deck at the abutment, pier 1, and pier 2. It can be seen that, for each earthquake, the response waveforms at these nodes were generally identical indicating that the fundamental effective mode dominated the response. The only exception to this observation was the response during the last 4 sec. of the Taft record. The displacement response of the pier foundations included visible contribution from higher modes in all cases especially for the Castaic record.

Comparison of the displacements for the static loads with those of the earthquake motions (Table 6.1) shows that, even though the nominal load was approximately the same for all cases (Ø.1g), no general trend existed between the displacements from static loads and displacements due to ground motions. The El Centro record led to maximum displacements which were from 1.6 to 8.2 times the static displacements while the displacements for the Taft record were from 1.4 to 6 times the static values. In contrast, the maximum displacements for Castaic were smaller than the static responses by factors ranging from Ø.34 to Ø.52.

Similar relationships exist between the static and dynamic internal forces (Table 6.2). The static loads caused pier base moments which were close but smaller than the corresponding cracking moments. The piers, however, cracked in both the El Centro and Taft input earthquakes leading in relatively significant nonlinear effects. The Castaic record resulted in forces which were considerably smaller than the static internal forces.

(b) Response for Measured Earthquake Records - The first 1Ø seconds of the measured corrected records for the earthquakes discussed in section 6.2 were used as input acceleration for the Rose Creek Bridge. The

PGA's were 0.35g for El Centro, 0.18g for Taft, and 0.35g for Castaic. The calculated response histories for one-half of the bridge are shown in Figs. 6.6-6.8, and the maximum responses are listed in Tables 6.3-6.5.

All three earthquakes resulted in the cracking of pier bases. The extent of cracking varied from one earthquake to the other. No yielding of reinforcement occurred during any of the earthquakes. Both the rotational and translational foundation springs for piers 1 and 4 experienced maximum deformations which exceeded the deformations corresponding to the first breakpoints in the primary curves. As a result, the overall stiffness of the bridge decreased significantly elongating the effective period. This is evident in the displacement histories of the deck (Figs. 6.6-6.8) when they are compared with the displacement histories due to earthquakes with PGA = 0.1g (Figs. 6.3-6.5).

In all cases, the effective fundamental mode dominated the response. Some residual displacement resulted in the deck at the intersection with pier 1 and, to a larger extent, pier 2 for the Castaic record (Fig. 6.8). The residual displacement can be explained as follows: both piers cracked at the base at approximately T = 3 sec. resulting in a relatively large displacement. Because the earthquake amplitudes became relatively small after this time, the large displacement could not be fully recovered; and, hence, the bridge oscillated about a new and shifted reference. The magnitude of the residual displacement in the abutments is considerably smaller because the abutment response is less sensitive to the cracking of piers. No major residual displacements occurred in the responses for the El Centro

and Taft records because these earthquakes included major acceleration pulses even after the maximum response took place which displaced the bridge back to its original position.

Comparison of the maximum displacements for different earthquakes (Table 6.3) shows that the El Centro record resulted in far greater displacements than the two other records. Part of the reason for the relatively large displacements for El Centro is the shift in the time axis (Fig. 6.6). Again, the Castaic record did not lead to any large displacements. The maximum forces and pier ductilities for this record were also smaller than those of the other two ground motions (Tables 6.4 and 6.5).

The maximum ductilities (defined as the maximum rotation divided by yield rotation) for the piers are all less than one indicating that none of the piers yielded in flexure.

Based on the maximum base moments, the maximum tensile force in the dowels was calculated. The stresses in the outermost steel layer in pier 2 were found to exceed the yield stress for both the El Centro and Taft earthquakes; although, because this layer was the only bar to reach its yield stress, the effective yield moment of the piers had not been reached. Based on both the 1963 and the 1983 ACI Codes [3], the dowels would not be able to develop their yield stress because of inadequate anchorage. Therefore, using the specified concrete and steel properties, one would conclude that the El Centro and Taft records would lead to the failure of the pier to pile-cap connections.

The magnitude of shear in pier 2 exceeded the nominal shear strength calculated based on the short formula from the 1983 ACI Code. Therefore, based on the analytical results, the middle two piers of the

bridge are likely to fail in shear if an earthquake similar to the 1940 El Centro earthquake occurs at the site of the Rose Creek Bridge. It should be noted, however, that, based on the Uniform Building Code and ATC-6 earthquake zone maps, such an earthquake is not considered likely to occur at the bridge site. Both the experimental and analytical results show that, for load levels specified by the code enforced at the time of design of this bridge, the strength is sufficient and a satisfactory performance of the bridge is expected.

CHAPTER 7

SUMMARY AND CONCLUSIONS

7.1 Summary

The purpose of the study presented in this report was to develop a nonlinear model for static and dynamic lateral response analysis of reinforced concrete highway bridges. The model allows for nonlinear behavior at deck to abutment connections, foundations, and pier bases. The bridge structures analyzed by the model were limited to those with single-column piers and those with no intermediate expansion joint. The connections between the piers and the deck were assumed to be monolithic. The response was considered only in the transverse direction of the bridge.

Two hysteresis models were incorporated in the model: the Ramberg-Osgood model and the trilinear Q-Hyst (TQ-Hyst) model. The latter is an expanded version of the Q-Hyst model and was developed to operate on a trilinear primary curve as opposed to a bilinear curve used in the Q-Hyst model. The model has the following analytical capabilities: (1) static analysis of the bridge for nodal horizontal loads, (2) free-vibration caused by initial displacements produced by quick release of horizontal static loads, and (3) earthquake response history analysis assuming that all the supports are subjected to the same input earthquake acceleration. The computer code implementing the model is called "ISADAB", standing for Inelastic Static and Dynamic Analysis of Bridges.

The analytical model was evaluated using the experimental data obtained from the testing of the Rose Creek Interchange Bridge, a five-span reinforced concrete bridge located near Winnemucca, Nevada. This

bridge was subjected to static and dynamic loads (using the quick-release method) in May 1982 to study its seismic behavior. The measured data used in the study presented in this report were those for static loads and the corresponding quick release of the loads with a magnitude of approximately one and one-half times the design loads. The extent of nonlinearity produced by these loads was limited. It was not, therefore, possible to evaluate the performance of the analytical model for medium and large amplitude loads which produce moderate and severe nonlinear effects. For the small amplitude responses which were used in the testing, the model appeared to lead to a reasonable estimate of the static response and free-vibration response histories provided realistic initial properties for the components are used.

The analytical model was used to determine and compare the deformations and internal forces of the bridge for the loads specified by the code in force at the time of the design of the bridge (AASHO 65) and by the new seismic code for bridges prepared by ATC-6. In addition, the model was used to evaluate the seismic performance of the Rose Creek Bridge subjected to three well known earthquake acceleration records each with two amplitudes; one normalized to 10 percent of gravity acceleration which was approximately equal to the loads applied in experimental studies, and the other with the actual measured peak acceleration for these records. The resulting displacements and internal forces were compared with each other and with the strength of the critical sections of the bridge.

7.2 Important Observations

In the process of developing the analytical model and utilizing it for the studies described in section 7.1, the following important

observations were made.

(a) Unlike the lateral response of multistory building structures subjected to lateral loads, which is ordinarily dominated by the structure and not the foundation, the bridge response can be sensitive to the stiffness characteristics of the abutments and foundations.

(b) In determining the initial properties of the elastomeric pads, it was found that the procedure specified by the manufacturer led to unreasonably small stiffnesses (based on the calculated displacements of the deck versus the measured values). The calculated stiffnesses from a system identification study of the bridge using the ambient vibration of the bridge [15] led to a reasonable estimate of displacements.

(c) The relatively close agreement between the analytical and the experimental results suggests that the overall modeling technique led to a reasonable representation of the actual system at least for low load levels (those producing only a small degree of nonlinearity).

(d) Because of the limited degree of nonlinearity in both the measured and the calculated results, it was not possible to comment on the performance of the analytical model for cases with severe nonlinearity. However, because the hysteresis models were based on the general characteristics of the measured response of bridge components obtained from the available literature, it can be stated that the analytical model is likely to be successful in reproducing the response of bridges with significant nonlinearity.

(e) The piers needed to be treated as uncracked elements to obtain a realistic estimate of the response.

(f) The distribution of internal forces for the Rose Creek Bridge based on the lollipop method was different from that based on the analysis of the total structure. The largest difference in forces was close to 30 percent.

(g) The comparison of internal forces based on AASHO 65 (pre-San Fernando earthquake code) and ATC-6 (post-San Fernando earthquake code) showed a significant increase in strength requirements in the new seismic guidelines. For the Rose Creek Bridge, the increase in shear forces was considerably more pronounced than that in moments.

(h) The calculated earthquake response of the Rose Creek Bridge with the maximum acceleration normalized to 10 percent of gravity (approximately the ultimate design load level) showed that the bridge was appropriately designed for the loads specified in the governing code.

7.3 Conclusions

The analytical studies presented in this report confirmed the results of previous findings that foundation and abutment bearing system flexibility play an important role in the seismic behavior of bridges. The degree of contribution of these elements to bridge flexibility, of course, depends on their properties as well as bridge properties (especially length and section properties of the piers). For ordinary highway bridges built as part of many highway interchanges, the influence of the foundations and the bearing system appear to be substantial.

The study showed that, before a realistic hysteresis model can be developed for elastomeric bearing pads, many more experimental results on the cyclic behavior of bearing pads are needed. Although not

directly substantiated, based on what has been learned for building structures, it is possible that the hysteresis modeling scheme has a significant influence on the nonlinear modeling of bridge systems. The Ramberg-Osgood hysteresis model appeared to be a reasonable model for bearing systems.

The newly adopted ATC-6 guidelines for the seismic design of highway bridges led to design internal forces for the Rose Creek Bridge which were considerably larger than those obtained using the AASHO 65 guidelines. The ATC-6 procedure was developed after the San Fernando earthquake during which many highway bridges were damaged or collapsed and after many studies on highway bridges and bridge components were conducted. The fact that the design forces based on ATC-6 are much greater than the pre-San Fernando earthquake loads can lead to the belief that bridges designed based on ATC-6 are likely to perform better in future earthquakes. Whether the load levels correspond to an optimum design in terms of economy and safety remains to be tested in future strong ground motions.

In earthquake response history studies of the Rose Creek Bridge, it was noted that different earthquakes had different effects on the bridge. The more common methods to determine the severity of the effect of an earthquake on structures are (1) to use the fundamental period of the system in conjuction with the earthquake response spectra, (2) to use the peak ground acceleration, and (3) to use the spectral intensity. None of these methods strictly applies to nonlinear systems. It appears that, to evaluate the seismic performance of bridge structures, it is necessary to analyze the bridge for a variety of earthquake records. The analysis cost and complexity of nonlinear models, of course, are

factors restricting the number of earthquake analyses that can be performed. To overcome this limitation, there appears to be a need for relatively simple nonlinear analytical models which can allow the designer to perform several analyses of the bridge rapidly and at a low cost.

REFERENCES

1. Alizadeh, M., and M.T. Davisson, "Lateral Load Tests on Piles - Arkansas River Project," Journal of Soil Mechanics and Foundations Divison, ASCE, Vol. 96, No. SM5, September 1970, pp. 1583-1604.

2. American Association of State Highway Officials, "Standard Specifications for Highway Bridges," Ninth Edition, 1965.

3. American Concrete Institute Committee 318, "Building Code Requirements for Reinforced Concrete (ACI 318-83)," Detroit, Michigan, 1977.

4. Applied Technology Council, "Seismic Design Guidelines for Highway Bridges," ATC-6, Berkeley, California, October 1981.

5. Chen, M. and J. Penzien, "Analytical Investigation of Seismic Response of Short, Single, or Multiple Span Highway Bridges," University of California, Berkeley, EERC Report No. 75-4, January 1975.

6. Clough, R.W., and J. Penzien, Dynamics of Structures, McGraw-Hill Book Co., 1975.

7. Davisson, M.T. and J.R. Salley, "Model Study of Laterally Loaded Piles," Journal of Soil Mechanics and Foundations Division, ASCE, Vol. 96, No. SM5, May 1970, pp. 1605-1627.

8. Derecho, A.T., S.K. Ghosh, M. Igbal, G.N. Freskakis, and M. Fintel, "Structural Walls in Earthquake-Resistant Buildings, Dynamic Analysis of Shear Walls, Parametric Studies," Portland Cement Association, Chicago, March 1978.

9. Douglas, B.M. and G.M. Norris, "Bridge Dynamic Tests/Implications for Seismic Design," ASCE Journal of Technical Topics, Vol. 101, No. 1, April 1983, pp. 1-22.

10. Douglas, B.M. and J.A. Richardson, "Maximum Amplitude Dynamic Tests of a Highway Bridge," Proceedings of the Eighth World Conference on Earthquake Engineering, San Francisco, July 1984.

11. Douglas, B.M., M. Saiidi, J.A. Richardson, and J.D. Hart, "Results from High-Amplitude Dynamic Tests and Implications for Seismic Design," Proceedings of the 15th Joint Meeting of U.S./Japan Panel on Wind and Seismic Effects, UJNR, May 1983.

12. Douglas, B.M. and W.H. Reid, "Dynamic Tests and System Identification of Bridges," Journal of the Structural Division, ASCE, Vol. 108, No. ST10, October 1982, pp. 2295-2312.

13. Duxin, H., "Earthquake Loading on Bridges," Proceedings of the First Conference on Computing in Civil Engineering, ASCE, 1978, pp. 262-273.

14. Gates, J.H., "Factors Considered in the Development of the California Seismic Design Criteria for Bridges," Proceedings of a Workshop on Earthquake Resistance of Highway Bridges, Applied Technology Council, November 1979, pp. 141-162.

15. Gates, J.H. and M.J. Smith, "Verification of Dynamic Modeling Methods by Prototype Excitation," California Department of Transportation, Report No. FHWA/CA/SD-82/07, 1982.

16. Ghee, A.B., M.J.N. Priestley, and R. Park, "Ductility of Reinforced Concrete Bridge Piers Under Seismic Loading," Report No. 81-3, Department of Civil Engineering, University of Canterbury, New Zealand, February 1981.

17. Gillies, A.G. and R. Shepherd, "Dynamic Inelastic Analysis of a Bridge Structure," Bulletin of the Seismological Society of America, Vol. 71, No. 2, April 1981, pp. 517-530.

18. Hart, J.D., "Nonlinear Modeling of Short Highway Bridges Subjected to Earthquake Loading," a thesis submitted in partial fulfillment of the requirements for the degree of Master of Science in Civil Engineering, University of Nevada, Reno, May 1984.

19. Hodson, K.E., Jr., "Simplified Inelastic Analysis of Reinforced Concrete Frame-Wall Structures Subjected to Earthquakes," a thesis submitted in partial fulfillment of the requirements for the degree of Master of Science in Civil Engineering, University of Nevada, Reno, May 1982.

20. Hognestad, E., "A Study of Combined Bending and Axial Load in Reinforced Concrete Members," Engineering Experimental Station, Bulletin Series No. 399, University of Illinois, Urbana, November 1951.

21. Imbsen, R.A., J. Lea, V.N. Kaliakin, K.J. Perano, J.H. Gates, and S.L. Perano, "SEISAB-1 Seismic Analysis of Bridges User's Manual," Engineering Computer Corporation, Sacramento, California, October 1982.

22. Imbsen, R.A. and R.A. Schamber, "Earthquake Resistant Bridge Bearings, Vol. 2 - NEABS Computer Program," U.S. Department of Transportation, Report No. FHWA/RD-82/166, Engineering Computer Corporation, Sacramento, California, May 1983.

23. Imbsen, R.A. and R.A. Schamber, "Energy Absorption and Stiffness Characteristics of Bridge Bearing Pads on Sliding Friction Surfaces Subjected to Dynamic Loadings with Varying Load Rates and Amplitudes," Interim Report to the FHWA, Engineering Computer Corporation, Sacramento, California, May 1981.

24. Imbsen, R.A., R.V. Nutt, and J. Penzien, "Evaluation of Analytical Procedures Used in Bridge Seismic Design Practice," Proceedings of a Workshop on Earthquake Resistance of Highway Bridges, Applied Technology Council, November 1979, pp. 476-496.

25. IMSL Library Reference Manual Ninth Edition, Houston, Texas, International Mathematical and Statistics Libraries, Inc., 1982.

26. Matlock, H., S. Foo, and L. Bryant, "Simulation of Lateral Pile Behavior Under Earthquake Motion, Earthquake Engineering and Soil Dynamics," Proceedings of the ASCE Geotechnical Engineering Division Specialty Conference, Vol. 2, Pasadena, California, ASCE, 1978.

27. Nachtrab, W.B. and R. Davidson, "Behavior of Elastomeric Bearing Pads Under Simultaneous Compression and Shear Loads," National Academy of Sciences - National Research Council, Highway Research Record No. 76, 1965, pp. 83-101.

28. Newmark, N.M., "A Method of Computation for Structural Dynamics," Journal of Engineering Mechanics Division, ASCE, Vol. 85, No. EM3, July 1959, p. 67-94.

29. Norris, G.M., "Lateral and Rotational Stiffness of Pile Foundations for the Seismic Analysis of Highway Bridges," CCEER Report, College of Engineering, University of Nevada, Reno, 1984, (In Preparation).

30. Otani, S., "SAKE, A Computer Program for Inelastic Response of R/C Frames to Earthquake," Civil Engineering Studies, Structural Research Series No. 413, University of Illinois, Urbana, November 1975.

31. Park, R., and T. Paulay, Reinforced Concrete Structures, John Wiley and Sons, Inc., 1975.

32. Penzien J., T. Iwasaki, and R.W. Clough, "Literature Survey-Seismic Effects on Highway Bridges," Report No. EERC 72-11, University of California, Berkeley, November 1972.

33. Poulous, H.G., "Behavior of Laterally Loaded Piles; 1) Single Piles, 2) Pile Groups," Journal of Soil Mechanics and Foundations Division, ASCE, Vol. 97, No. SM5, May 1971, pp. 711-751.

34. Price, G., "Field Tests on Vertical Piles Under Static and Cyclic Horizontal Loading in Overconsolidated Clay," ASTM, STP 670, 1979, pp. 464-483.

35. Priestly, M.J.N. and R. Park, "Seismic Resistance of Reinforced Concrete Bridge Columns," Proceedings of a Workshop on Earthquake Resistance of Highway Bridges, Applied Technology Council, November 1979, pp. 253-284.

36. Ramberg, W. and W.T. Osgood, "Description of Stress-Strain Curves by Three Parameters," NACA Technical Note No. 902, 1943.

37. Saiidi, M. and B.M. Douglas, "Effect of Design Seismic Loads on a Highway Bridge," accepted for publication in the Journal of Structural Engineering, ASCE, to be published in November 1984.

38. Saiidi, M. and J.D. Hart, "Nonlinear Seismic Response of Short Reinforced Concrete Highway Bridges," Proceedings of the Eighth World Conference on Earthquake Engineering, San Francisco, July 1984.

39. Saiidi, M. and M.A. Sozen, "Simple and Complex Models for Nonlinear Seismic Response of Reinforced Concrete Structures," Structural Research Series No. 465, Civil Engineering Studies, University of Illinois, Urbana, August 1979.

40. Saiidi, M., "Hysteresis Models for Reinforced Concrete," Journal of the Structural Division, ASCE, Vol. 108, No. ST5, May 1982, pp. 1077-1085.

41. Saiidi, M., "Influence of Hysteresis Models on Calculated Seismic Response of Reinforced Concrete Structures," Proceedings of the Seventh World Conference in Earthquake Engineering, Istanbul, Turkey, Vol. 5, September 1980, pp. 423-430.

42. Takeda, T., M.A. Sozen, and N.N. Nielson, "Reinforced Concrete Response to Simulated Earthquakes," Journal of the Structural Division, ASCE, Vol. 96, No. ST12, December 1970, pp. 2557-2573.

TABLE 4.1 - PRIMARY CURVE PROPERTIES FOR ELEMENTS OF THE ROSE CREEK BRIDGE

	FORCE AT BREAKPOINT			DEFORMATION AT BREAKPOINT		
UNITS: KIPS, INCHES, RADIANS	1	2	3	1	2	3
Interior Pier Bases-- Moment-Curvature Bond Slip Rotation	21,790.	53,750.	56,500.	.648 E-6 0	.504 E-3 .358 E-4	.12 E-2 .396 E-3
Exterior Pier Bases-- Moment-Curvature Bond Slip Rotation	27,960.	61,700.	65,100.	.665 E-5 0	.54 E-3 .358 E-4	.12 E-2 .398 E-3
Interior Pile Caps-- Force-Displacement	90.	198.	278.	.053	.29	1.0
Exterior Pile Caps-- Force-Displacement	278.	585.	792.	.053	.325	1.0
Interior Pile Caps-- Moment-Rotation	23,000.	40,000.	45,000.	.5 E-3	.148 E-2	.42 E-2
Exterior Pile Caps-- Moment-Rotation	50,000.	102,000.	115,000.	.5 E-3	.197 E-2	.38 E-2
Abutment-- Moment-Rotation About Vertical Axis	2892.	-----	-----	.01	-----	-----
Abutment-- Moment-Rotation About Deck Axis	2440.	-----	-----	.419 E-3	-----	-----
Abutment-- Force-Displacement	23.	-----	-----	.0628	-----	-----

TABLE 4.2 - PIER FORCES FOR AASHO-65 LOADS

	(a) (Lollipop Method)		(b) (Total Structure)	
	Base Mom. (k-ft)	Shear (k)	Base Mom. (k-ft)	Shear (k)
Pier 1	1,002	47.7	757	33.9
Pier 2	1,257	59.6	1,296	63.7

TABLE 4.3 - ATC-6 DESIGN PARAMETERS

$\alpha = \int V_S \, dx = 2.19$	ft^2
$\beta = \int W V_S \, dx = 23.2$	kip-ft
$\gamma = \int W V_S^2 \, dx = 0.150$	$kip\text{-}ft^2$
Fundamental Period = 0.29	Sec.
$C_S = 1.2AS/T^{2/3} = 0.525$*	
$P_e/V_S = 859$	kip/ft
$P_e/W = 0.44$	

*Upper limit on C_S controlled

Parameters:

P_e = equivalent static seismic load;
S = site response coefficient;
T = bridge period;
V_S = static displacement due to uniform load;
W = bridge dead load.

TABLE 4.4 - PIER FORCES FOR ATC-6 LOADS

	Elastic		Inelastic	
	Base Mom. (k-ft)	Shear (k)	Base Mom. (k-ft)	Shear (k)
Pier 1	2,086	234	2,146	287
Pier 2	4,677	624	3,280	482

TABLE 4.5 - PIER FORCES BASED ON THE OLD AND NEW CODES

	AASHO (1965)		ATC-6 (1981)	
	Base Mom. (k-ft)	Shear (k)	Base Mom. (k-ft)	Shear (k)
Pier 1	1,403	66.8	2,086	234
Pier 2	1,760	83.4	4,677	624

TABLE 6.1 - MAXIMUM ABSOLUTE DISPLACEMENTS FOR STATIC LOADS AND EARTHQUAKES WITH PGA = 0.1G

Load	North Abut.	Pier 1	Pier Base 1	Pier 2	Pier Base 2
Static	0.117	0.152	0.029	0.162	0.018
El Centro NS	0.563	0.799	0.096	1.33	0.029
Taft S69E	0.381	0.604	0.062	0.981	0.026
Castaic N21E	0.047	0.051	0.015	0.051	0.009

unit = inches

TABLE 6.2 - MAXIMUM ABSOLUTE INTERNAL FORCES FOR STATIC LOADS AND EARTHQUAKES WITH PGA = 0.1G

Load	Lateral Abut. Force	Pier 1 Base Mom.	Pier 1 Shear	Pier 2 Base Mom.	Pier 2 Shear
Static	21.8	14,020	50.4	26,700	86.8
El Centro NS	73.8	23,910	84.7	31,070	126.5
Taft S69E	54.4	22,390	81.3	29,420	116.0
Castaic N21E	10.5	5,153	18.8	8,726	31.1

unit = kips and inches

TABLE 6.3 - MAXIMUM ABSOLUTE DISPLACEMENTS FOR MEASURED EARTHQUAKE RECORDS

Earthquake	North Abut.	Pier 1	Pier Base 1	Pier 2	Pier Base 2
El Centro NS	2.35	3.09	0.154	4.16	0.049
Taft S69E	0.87	1.0	0.103	1.37	0.032
Castaic N21E	0.16	0.29	0.075	0.51	0.029

unit = inches

TABLE 6.4 - MAXIMUM ABSOLUTE INTERNAL FORCES FOR MEASURED EARTHQUAKE RECORDS

Earthquake	Lateral Abut. Force	Pier 1 Base Mom.	Pier 1 Shear	Pier 2 Base Mom.	Pier 2 Shear
El Centro NS	212.9	26,500	116.7	32,410	214.4
Taft S69E	102.7	24,170	93.7	32,250	152.2
Castaic N21E	28.5	22,020	71.0	28,730	108.1

unit = kips and inches

TABLE 6.5 - MAXIMUM PIER DUCTILITIES FOR MEASURED EARTHQUAKE RECORDS

Earthquake	Pier 1	PIER 2
El Centro NS	Ø.37	Ø.39
Taft S69E	Ø.31	Ø.39
Castaic N21E	Ø.26	Ø.31

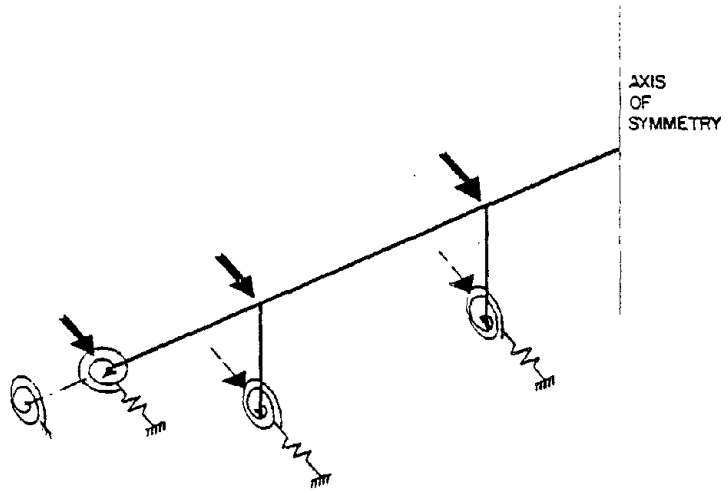

Fig. 2.1 Schematic View of One-Half of a Bridge System

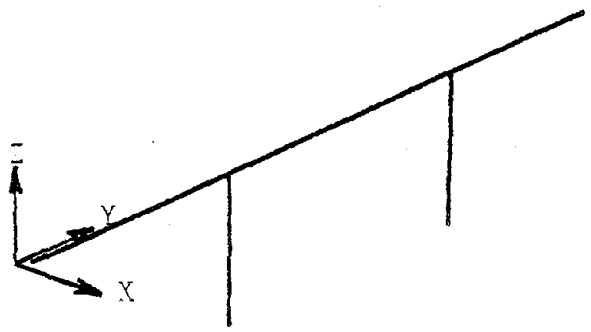

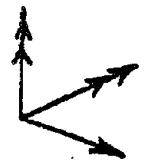

Deck Nodes

Pier Base Nodes

Fig. 2.2 Permissible DOF's

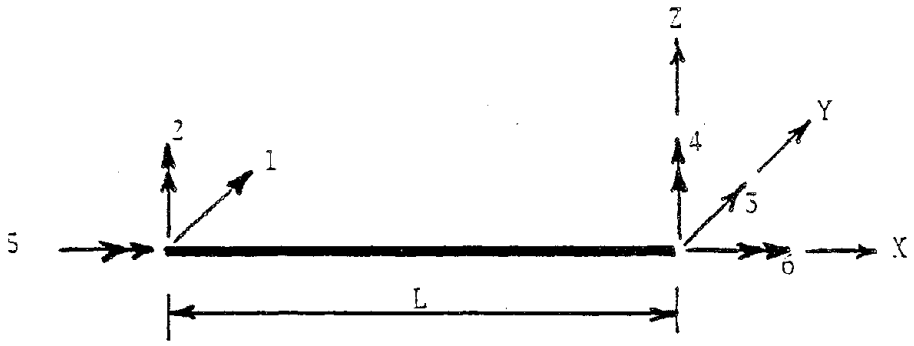

Fig. 2.3 Degrees of Freedom for a Deck Element

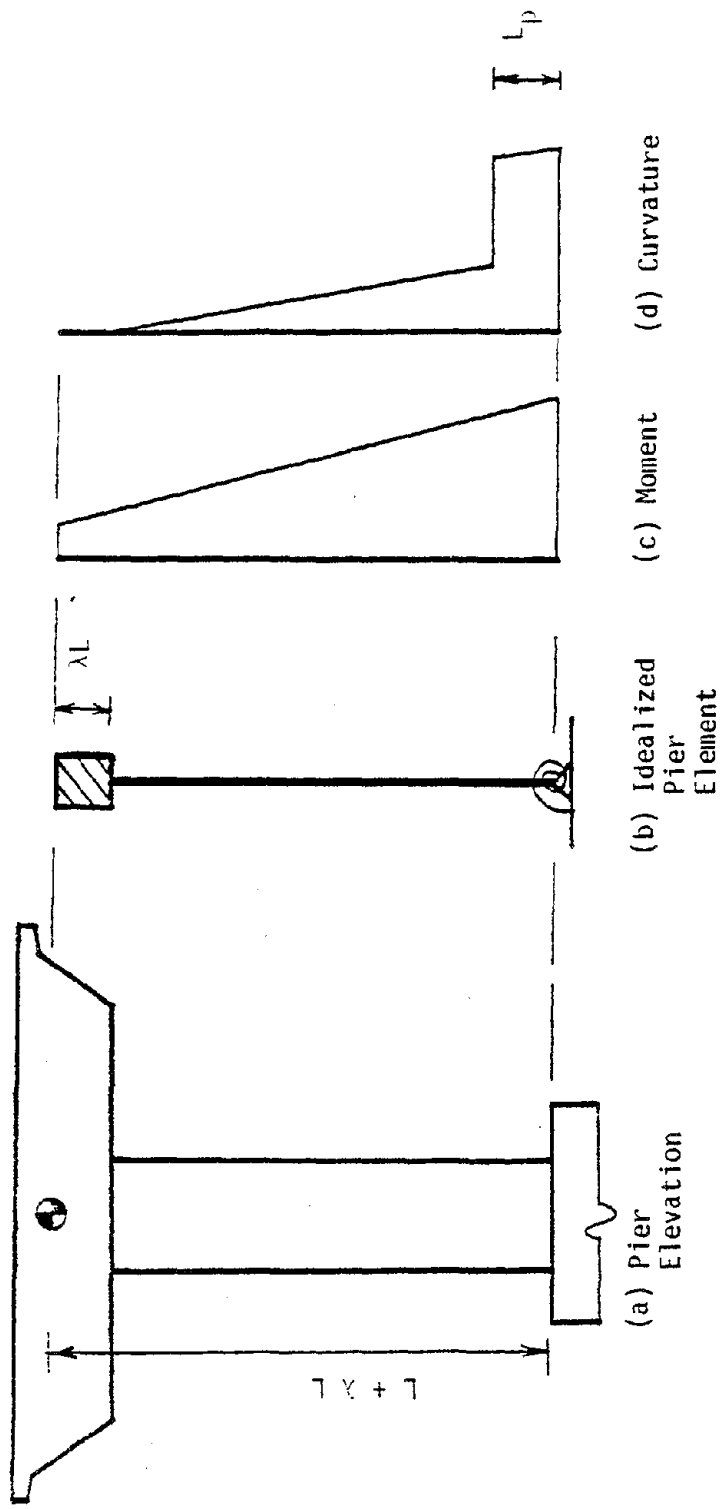

Fig. 2.4 Pier Element

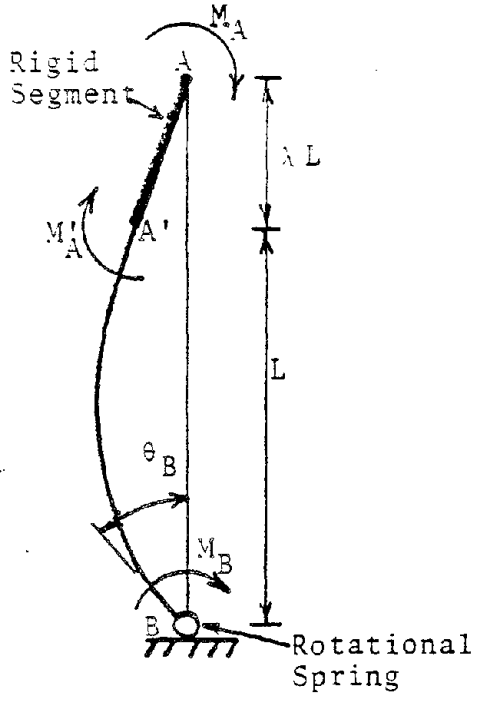

Fig. 2.5 Deformed Shape of a Pier Element (No Lateral Disp.)

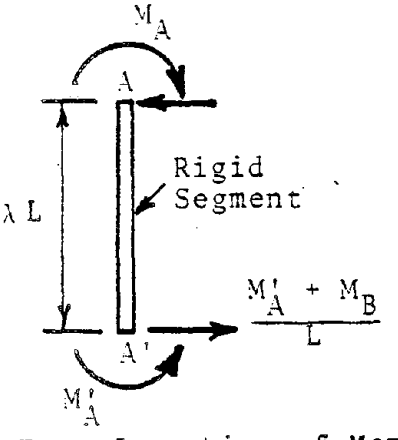

Fig. 2.6 Transformation of Moments for the Rigid Segment

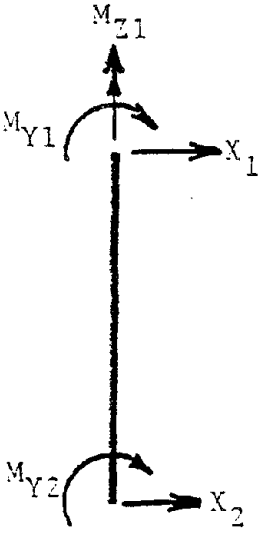

Fig. 2.7 Permissible DOF's for Pier Elements

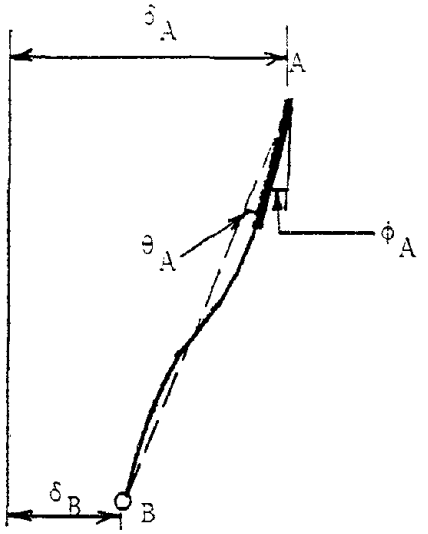

Fig. 2.8 Deformed Shape of a Pier Element (With Lateral Disp.)

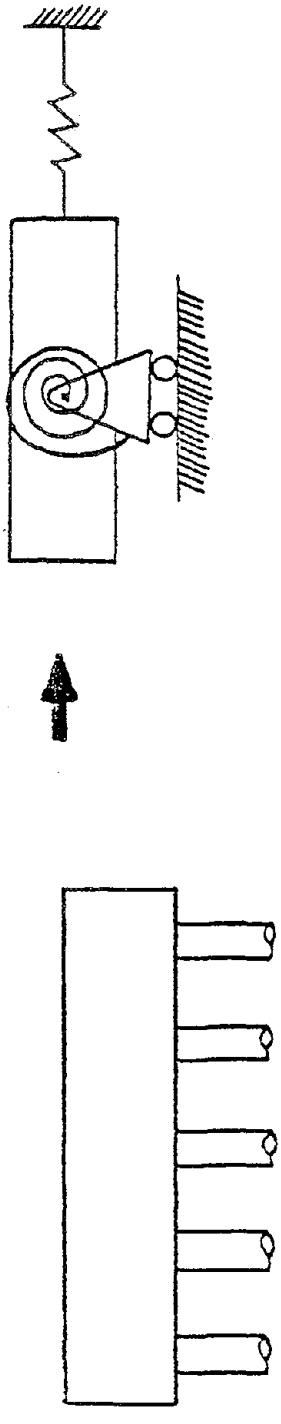

Fig. 2.9 Idealization of Foundation

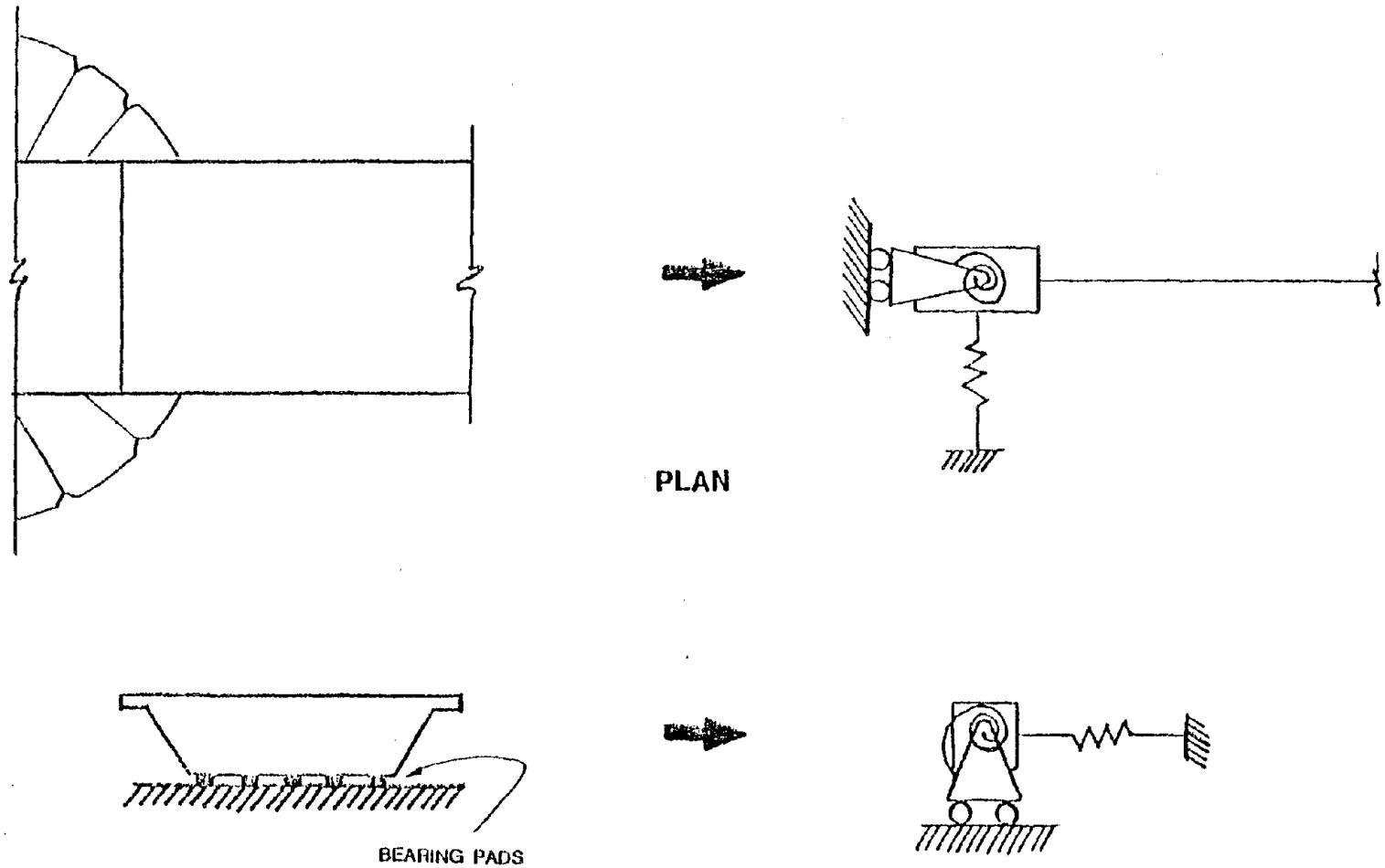

Fig. 2.1Ø Idealization of Abutments

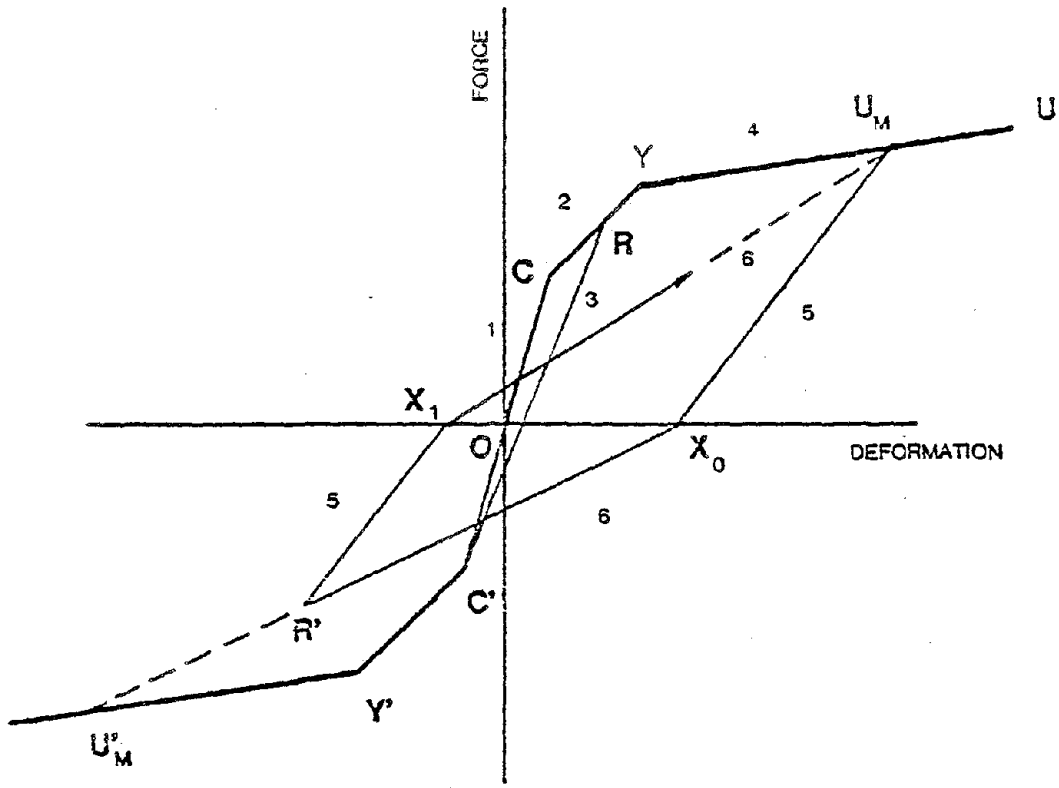

Fig. 2.11 The TQ-Hyst Model

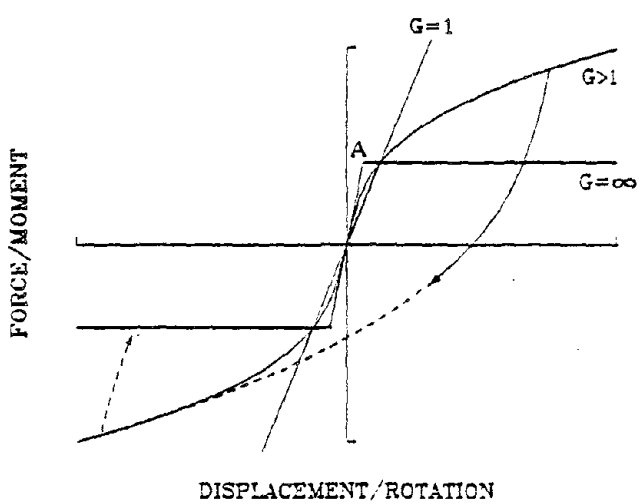

Fig. 2.12 The Ramberg-Osgood Hysteresis Model

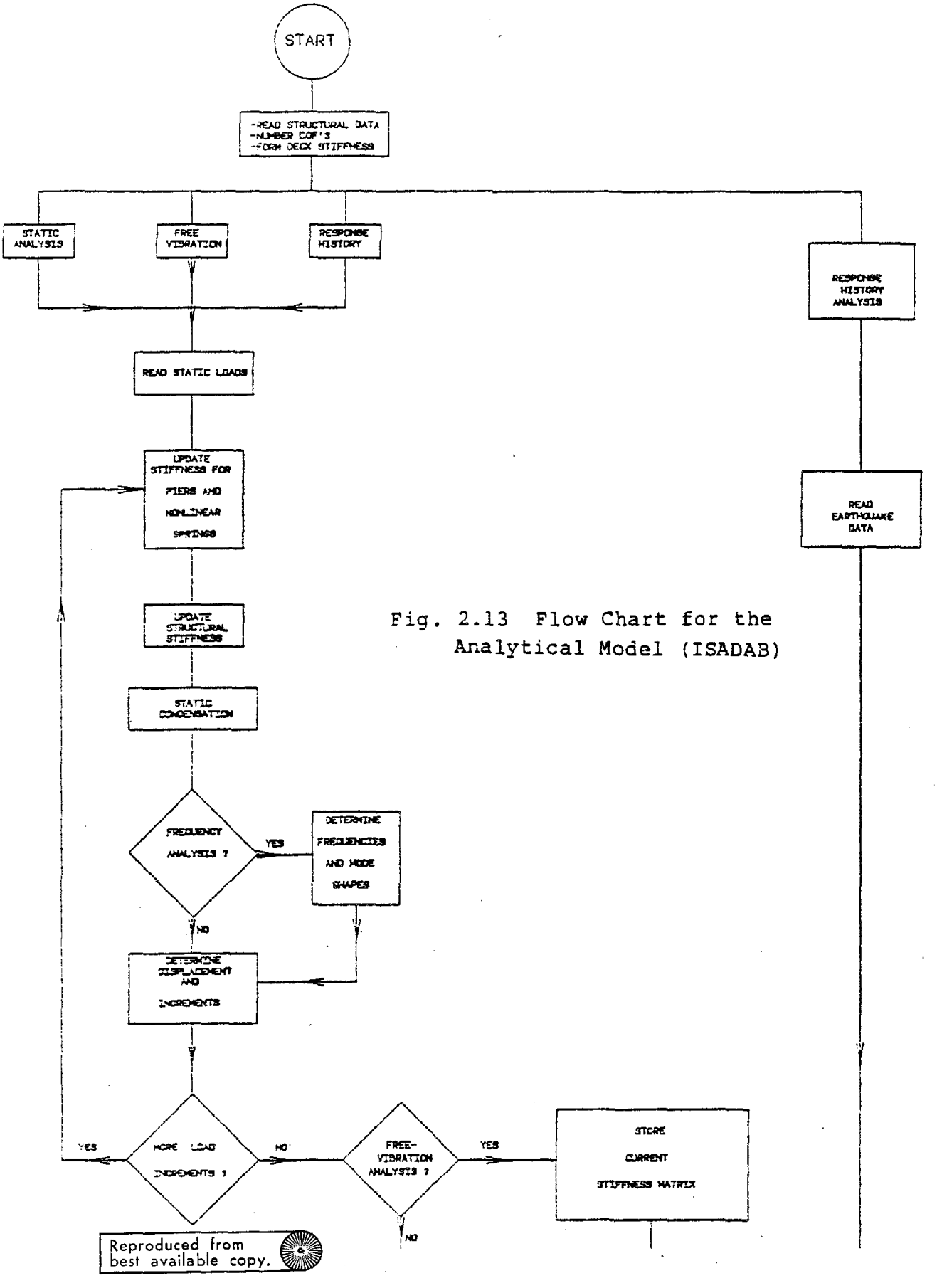

Fig. 2.13 Flow Chart for the Analytical Model (ISADAB)

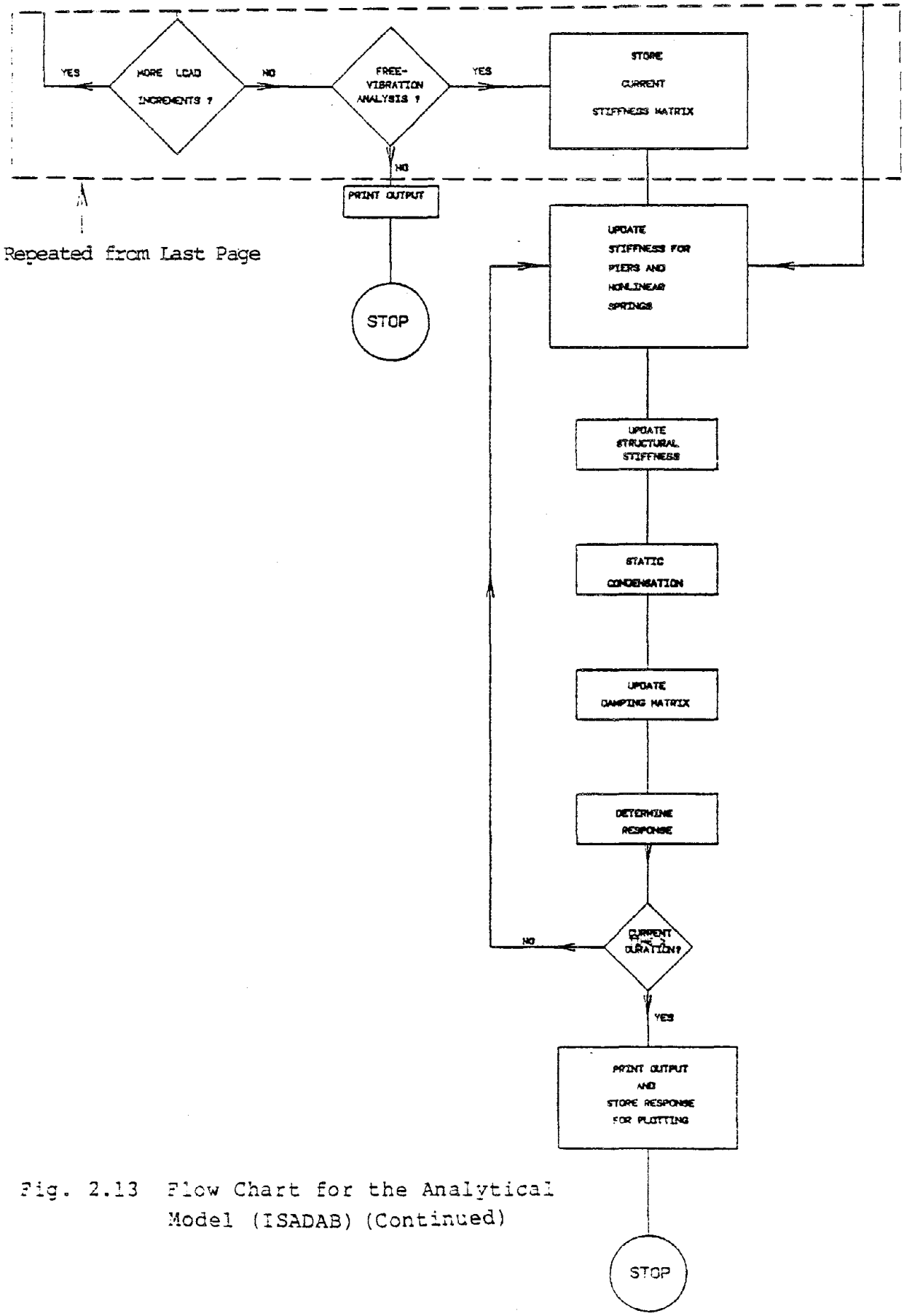

Fig. 2.13 Flow Chart for the Analytical Model (ISADAB) (Continued)

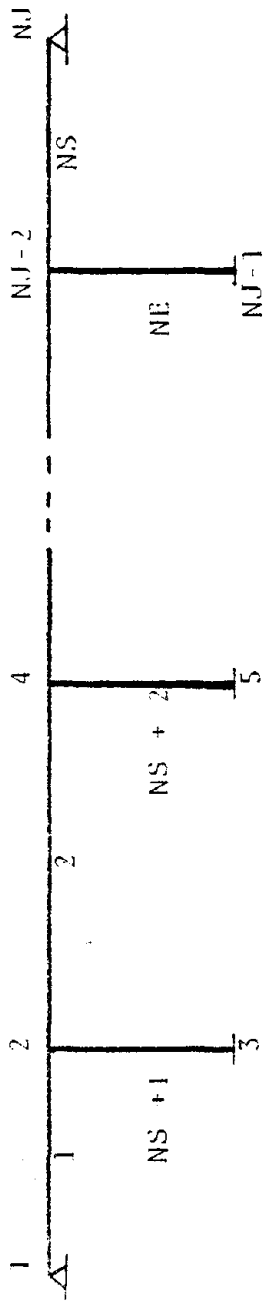

Fig. 2.14 Node Numbering Scheme

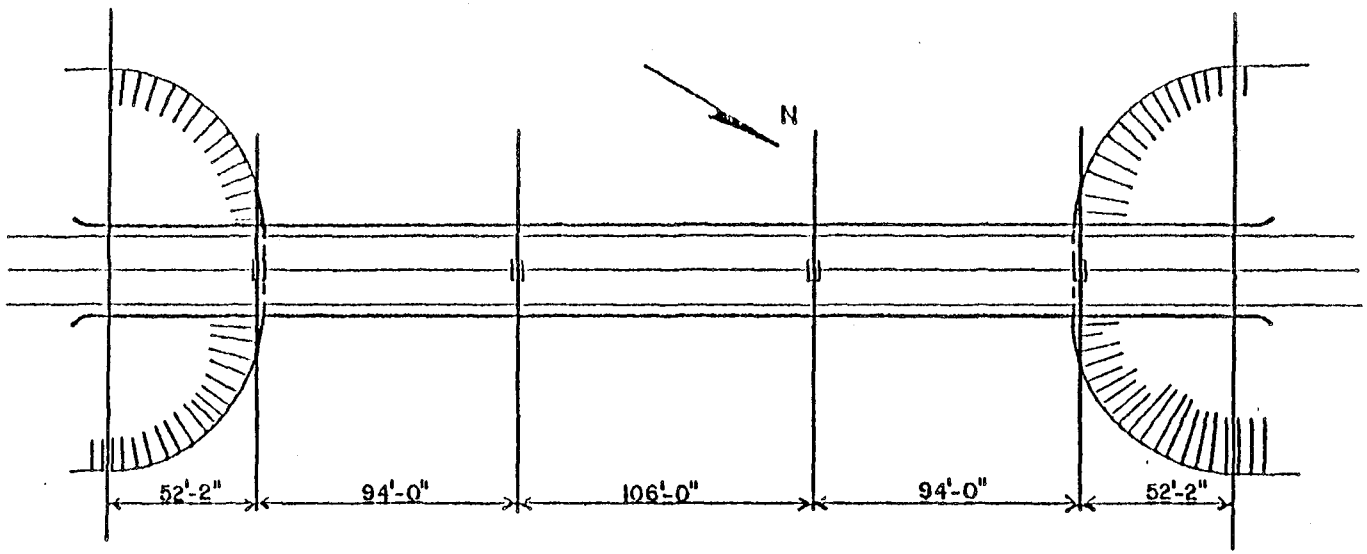

PLAN

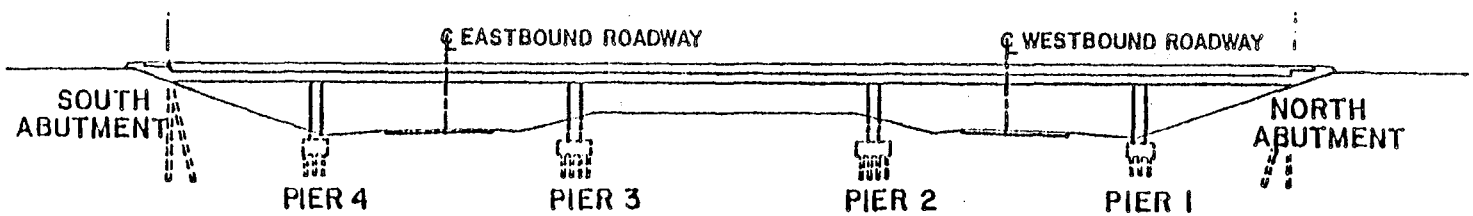

ELEVATION NORMAL TO FREEWAY

Fig. 3.1 Planview and Elevation of Rose Creek Bridge

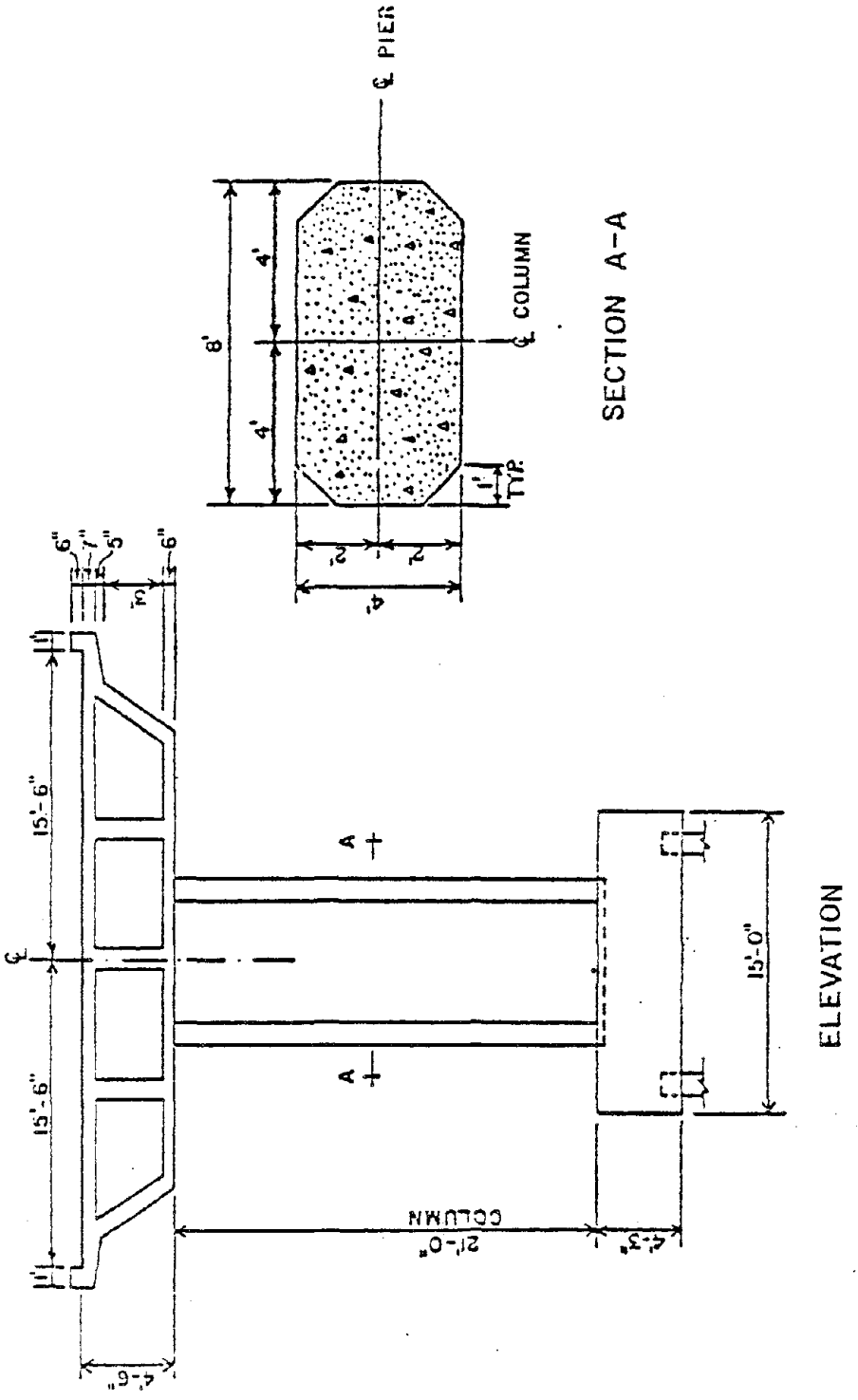

Fig. 3.2 Pier Elevation

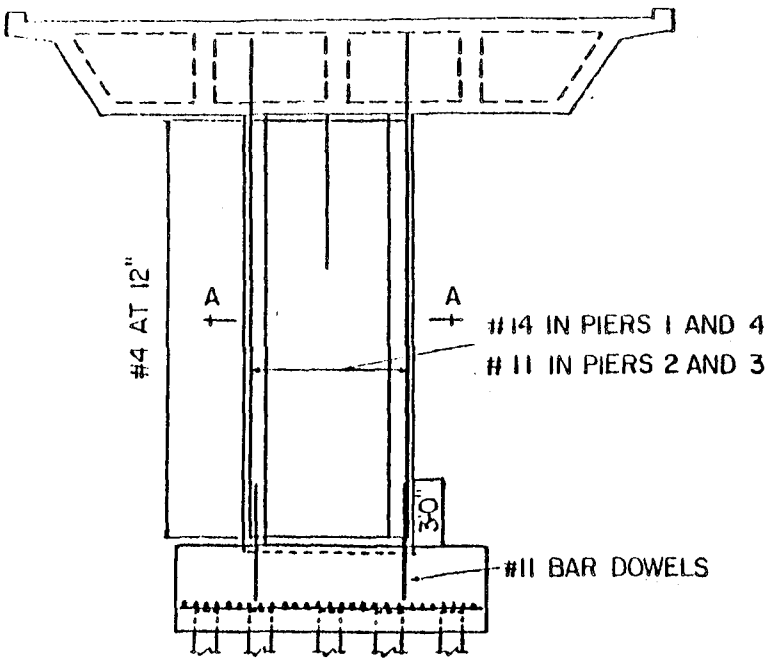

ELEVATION

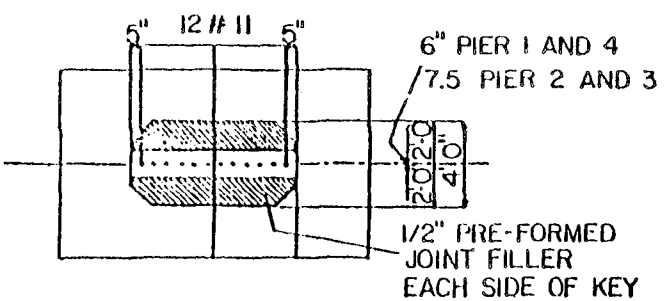

FOOTING PLAN

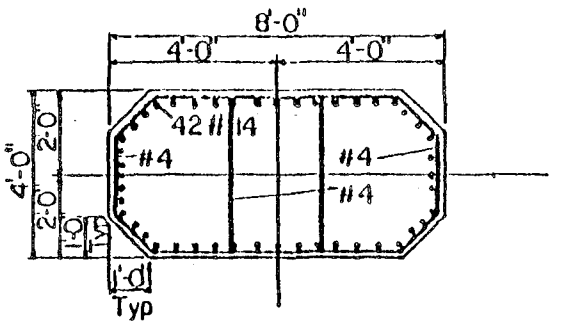

SECTION A-A FOR PIER 1 AND 4

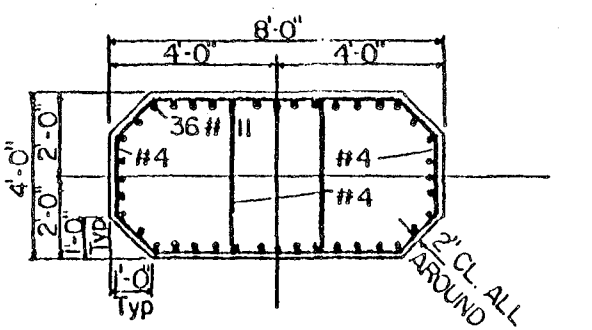

SECTION A-A FOR PIER 2 AND 3

Fig. 3.3 Pier Reinforcement

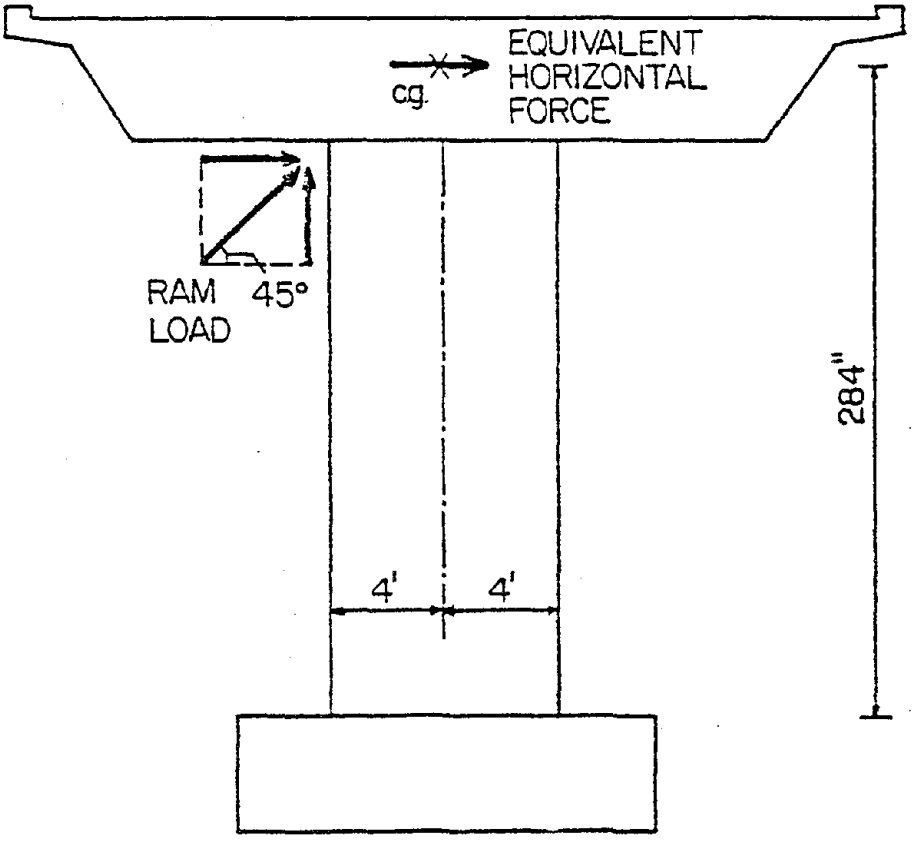

Fig. 3.4 Ram Load and the Equivalent Horizontal Force

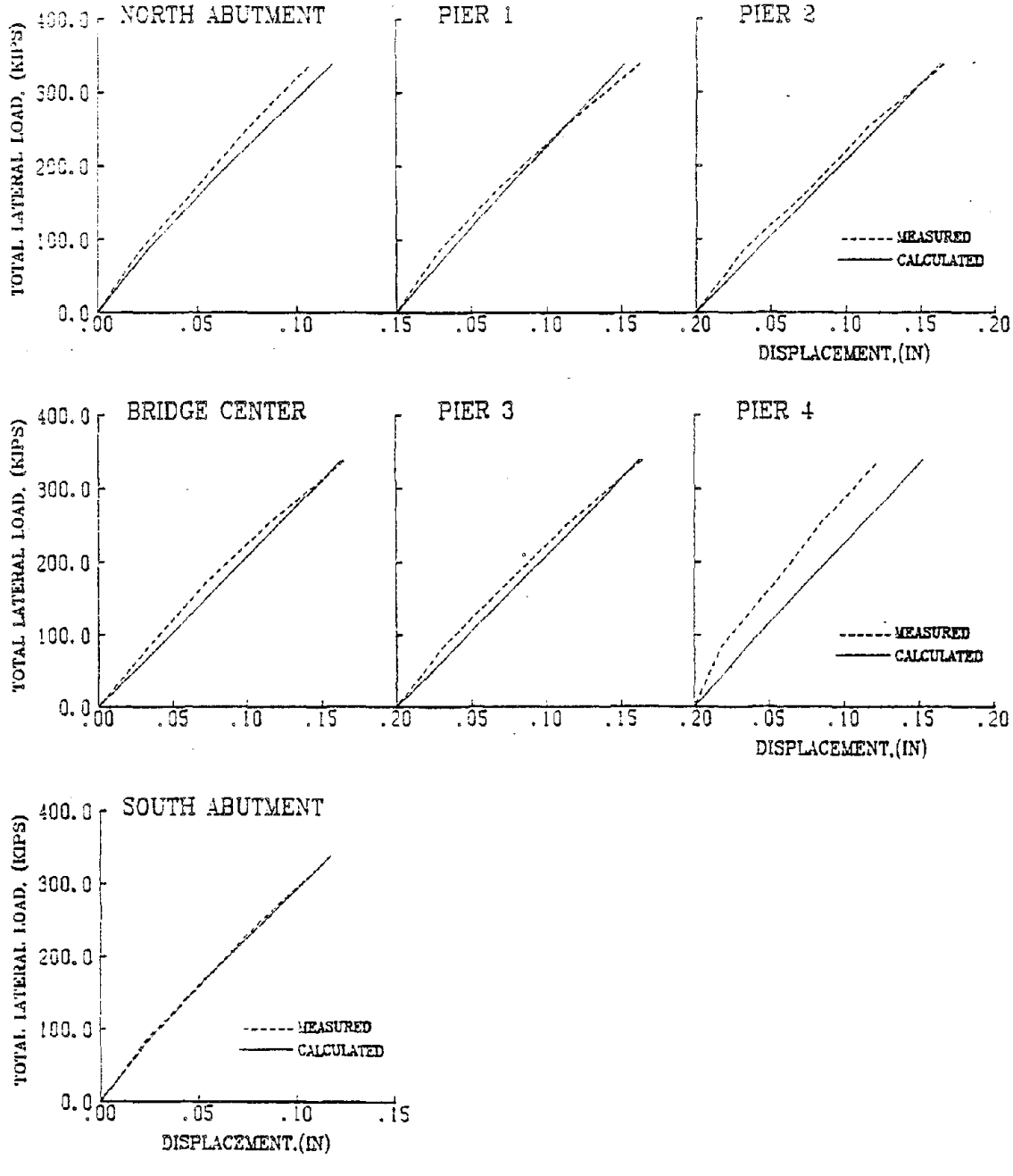

Fig. 4.1 Force-Displacement Relationships for Static Loads

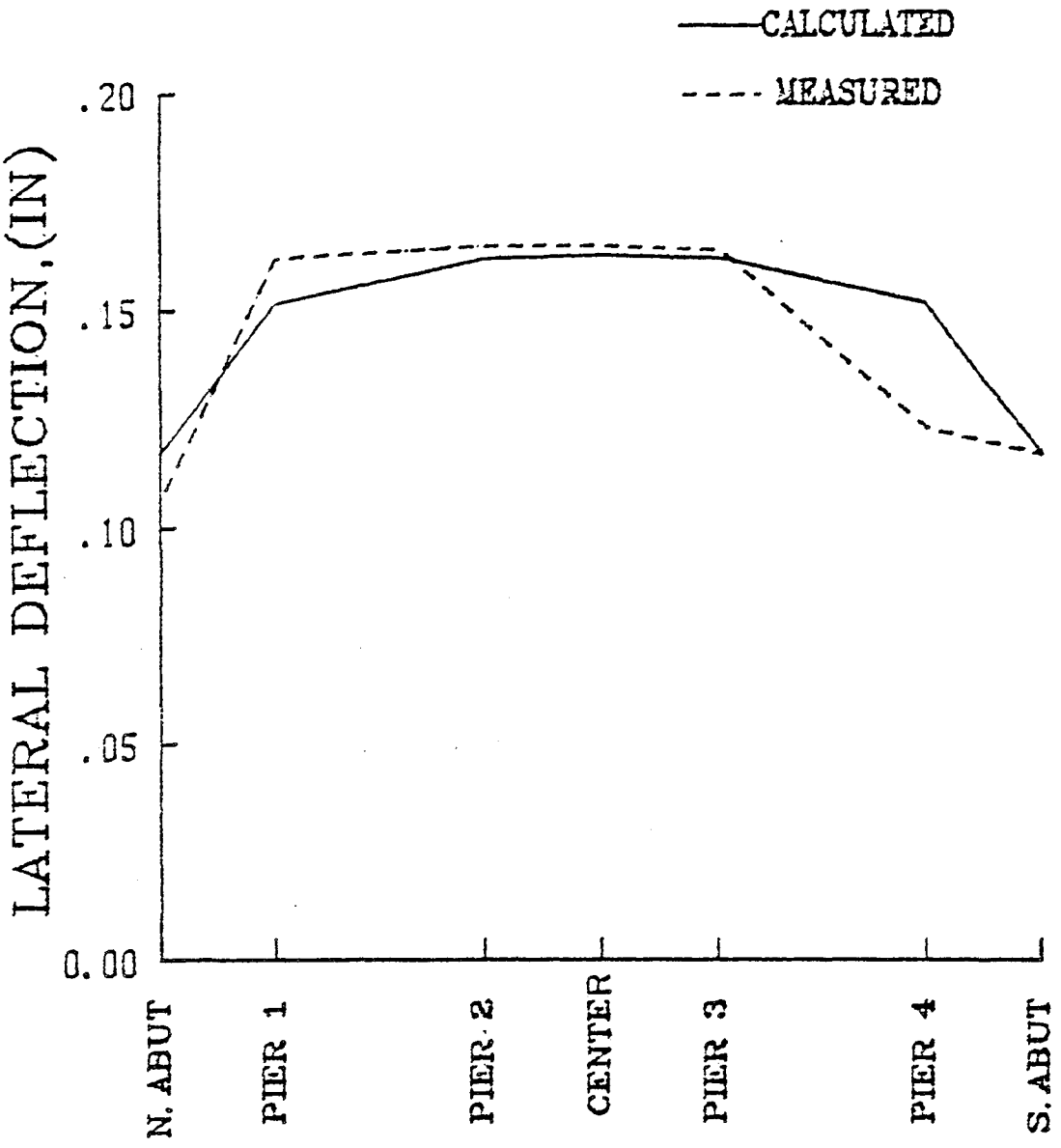

Fig. 4.2 Deck Deflection at Maximum Test Load

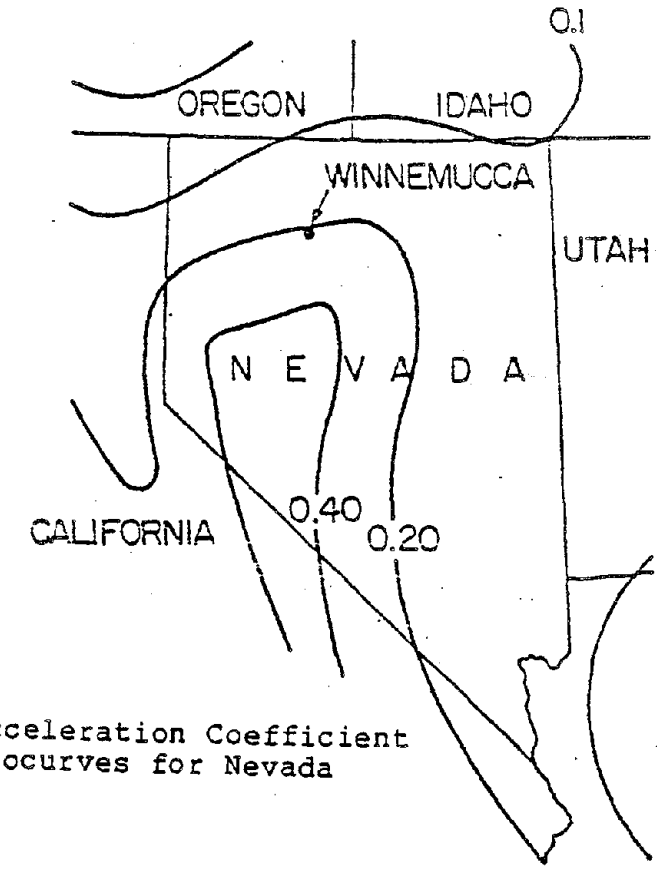

Fig. 4.3 Acceleration Coefficient Isocurves for Nevada

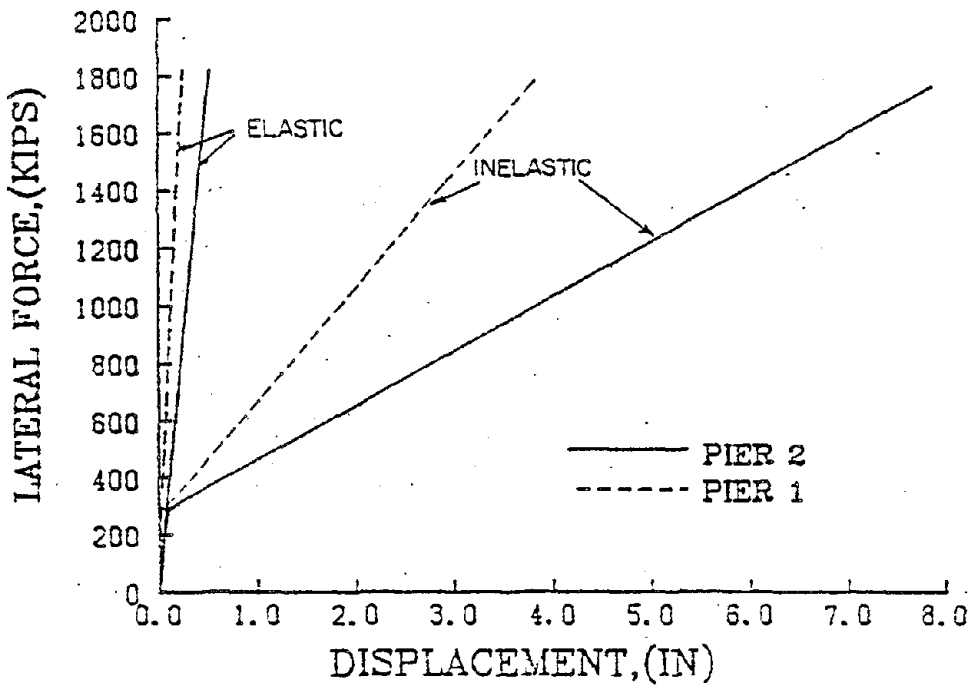

Fig. 4.4 Force-Displacement Response for ATC-6 Loads

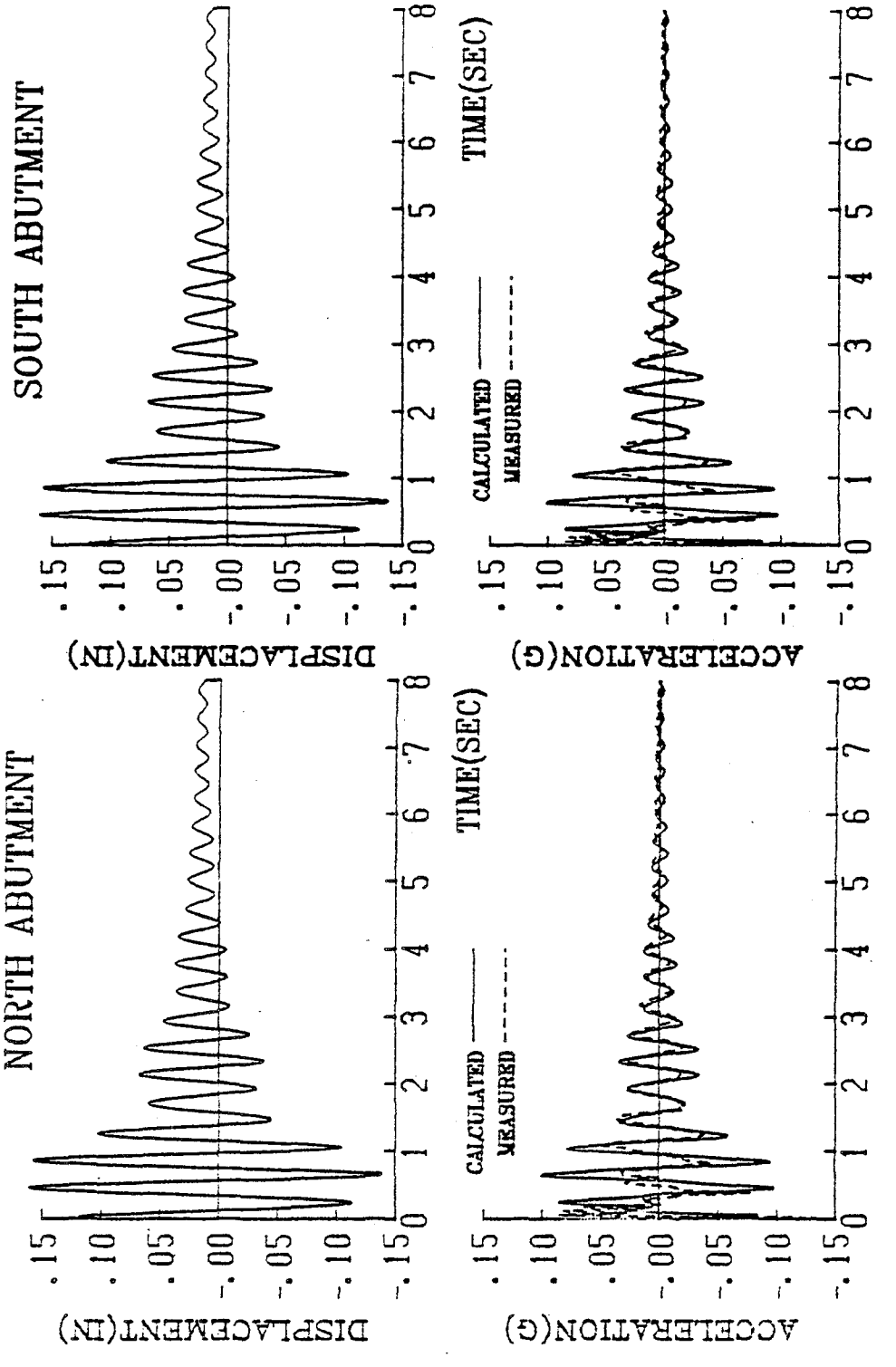

Fig. 5.1 Free-Vibration Response of the Abutments

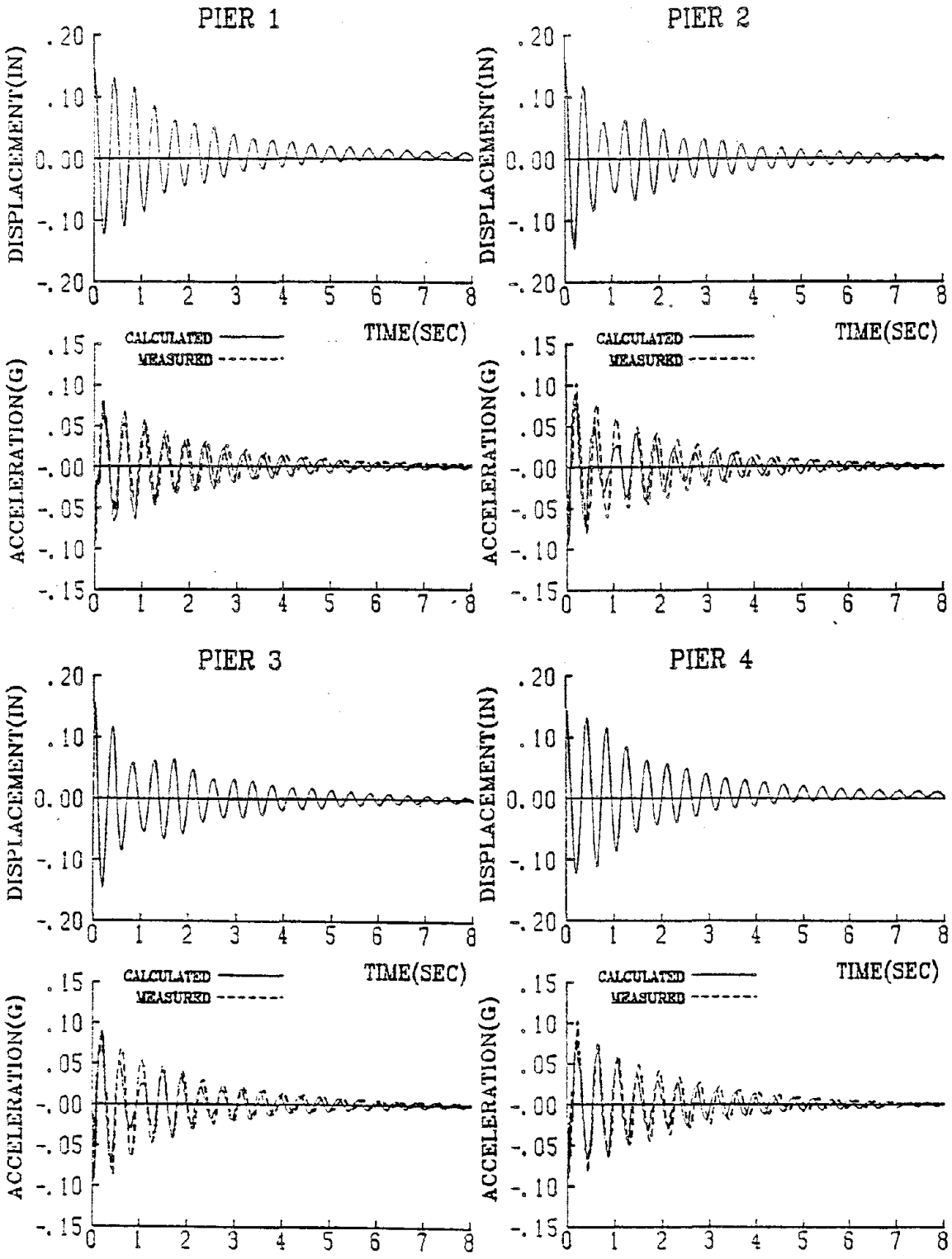

Fig. 5.2 Free-Vibration Response of the Deck at Pier Tops

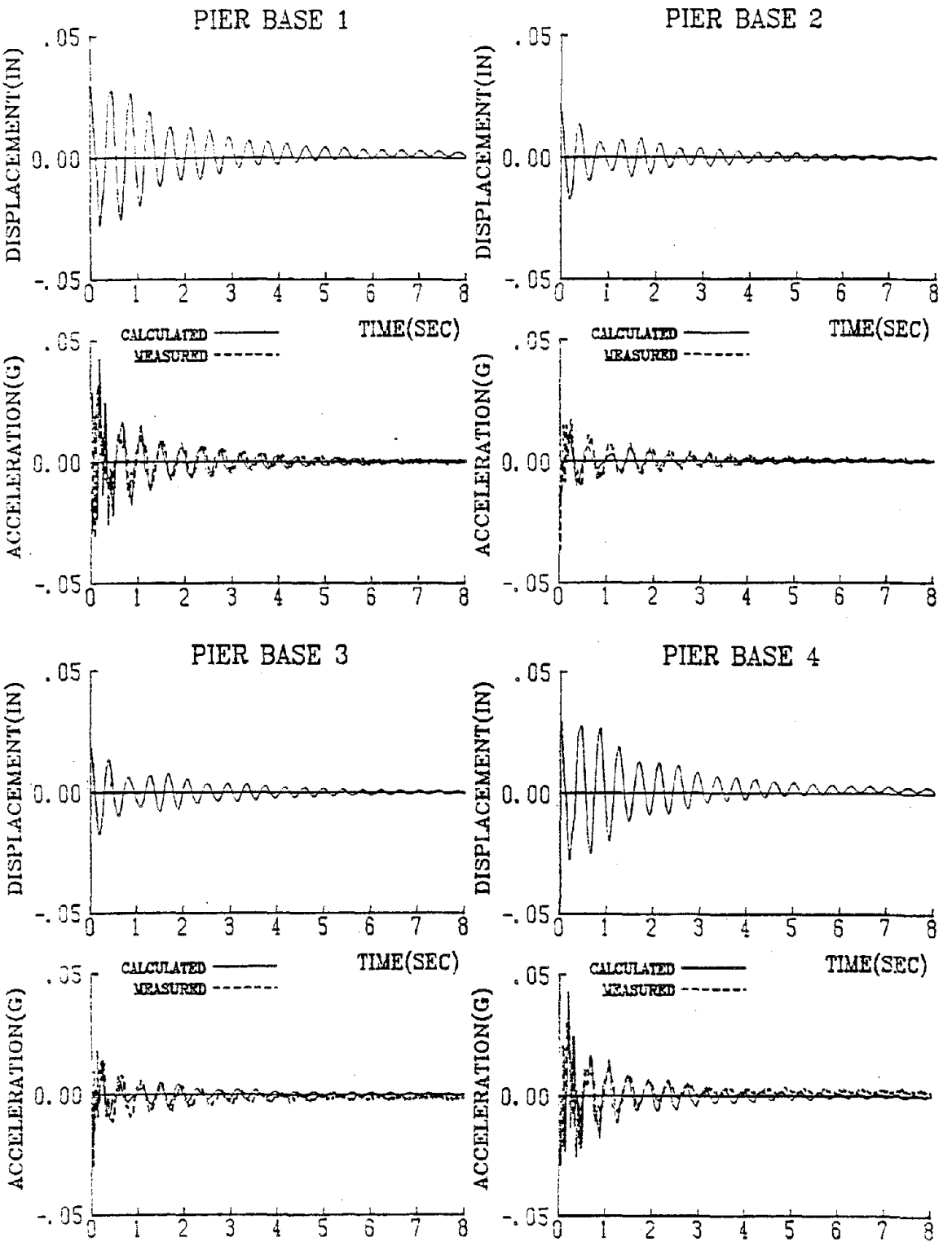

Fig. 5.3 Free-Vibration Response of Pier Foundations

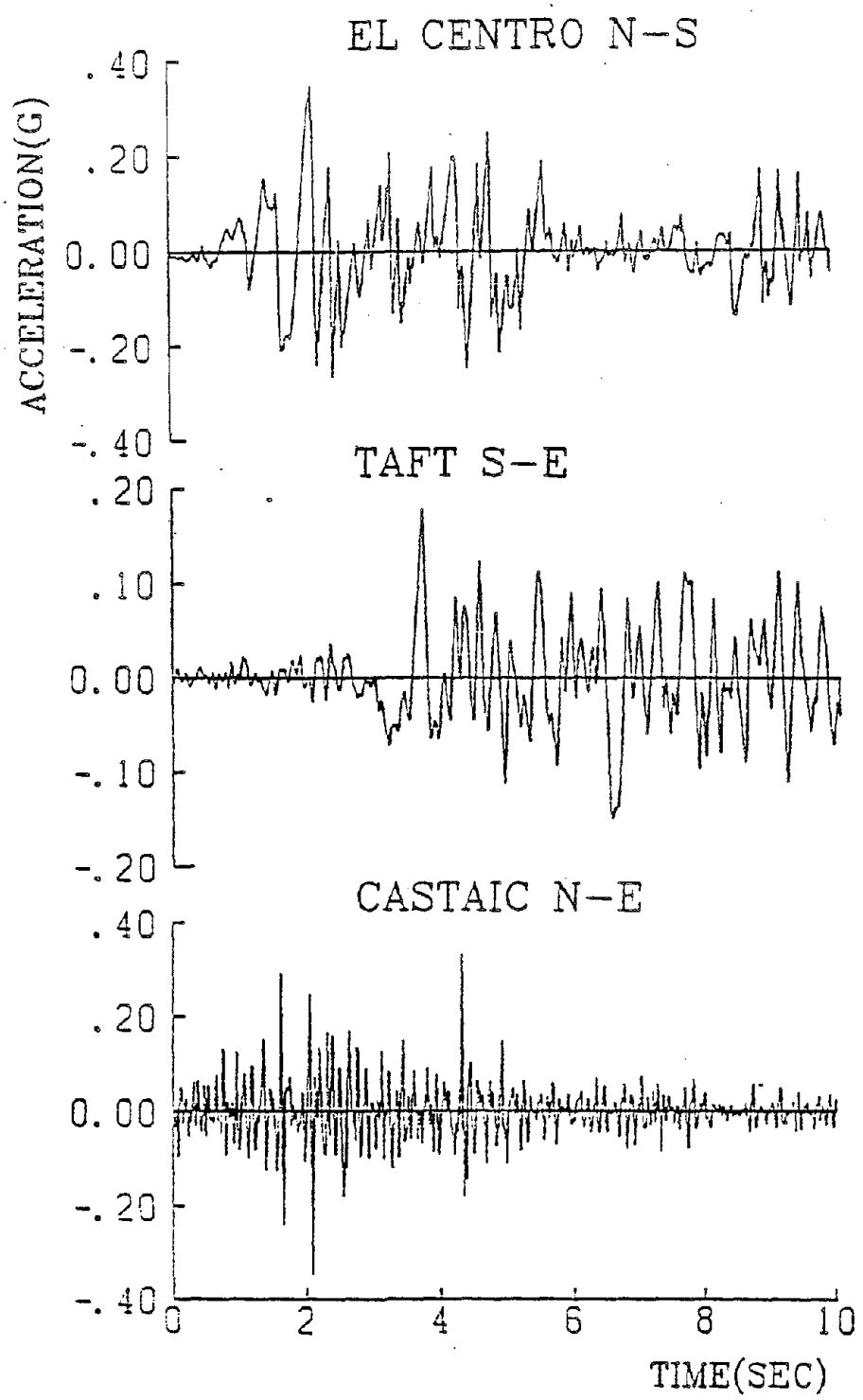

Fig. 6.1 Acceleration Records for Input Earthquakes

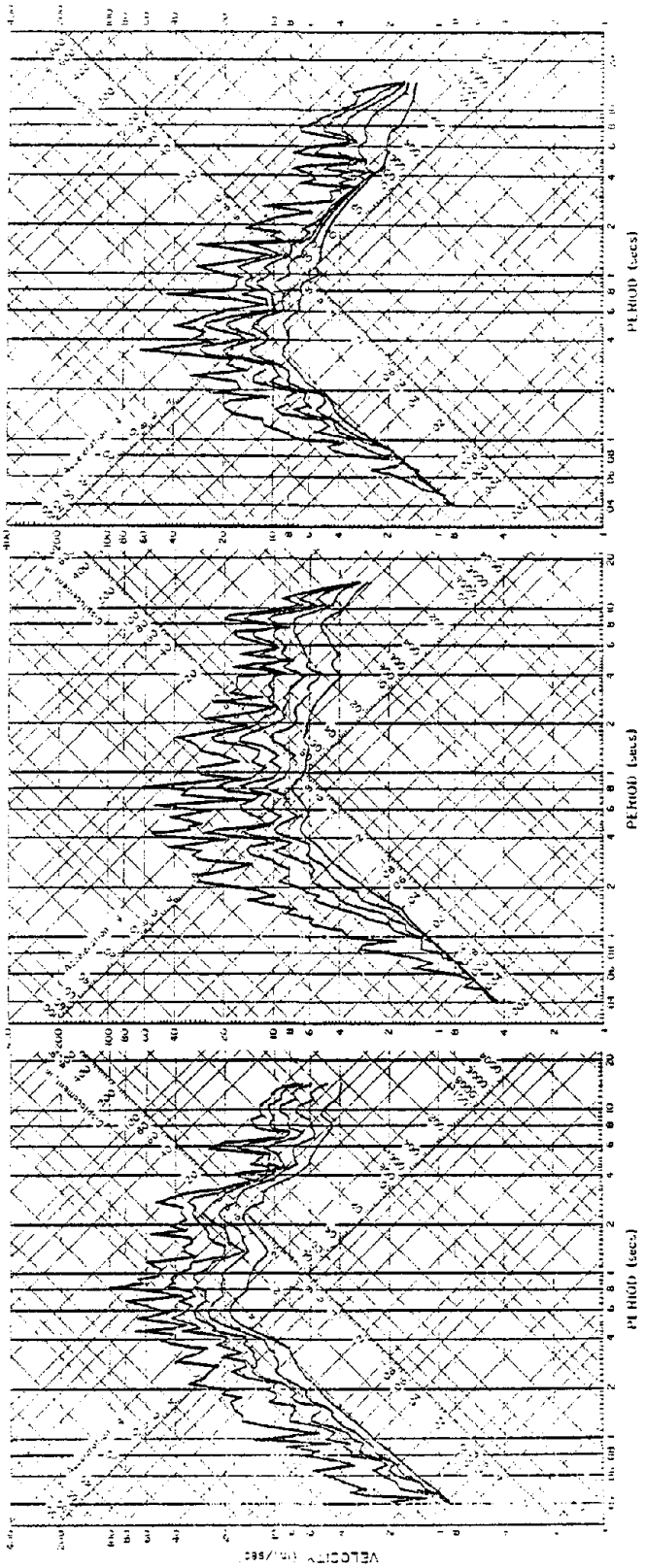

Fig. 6.2 Response Spectra for Input Earthquakes

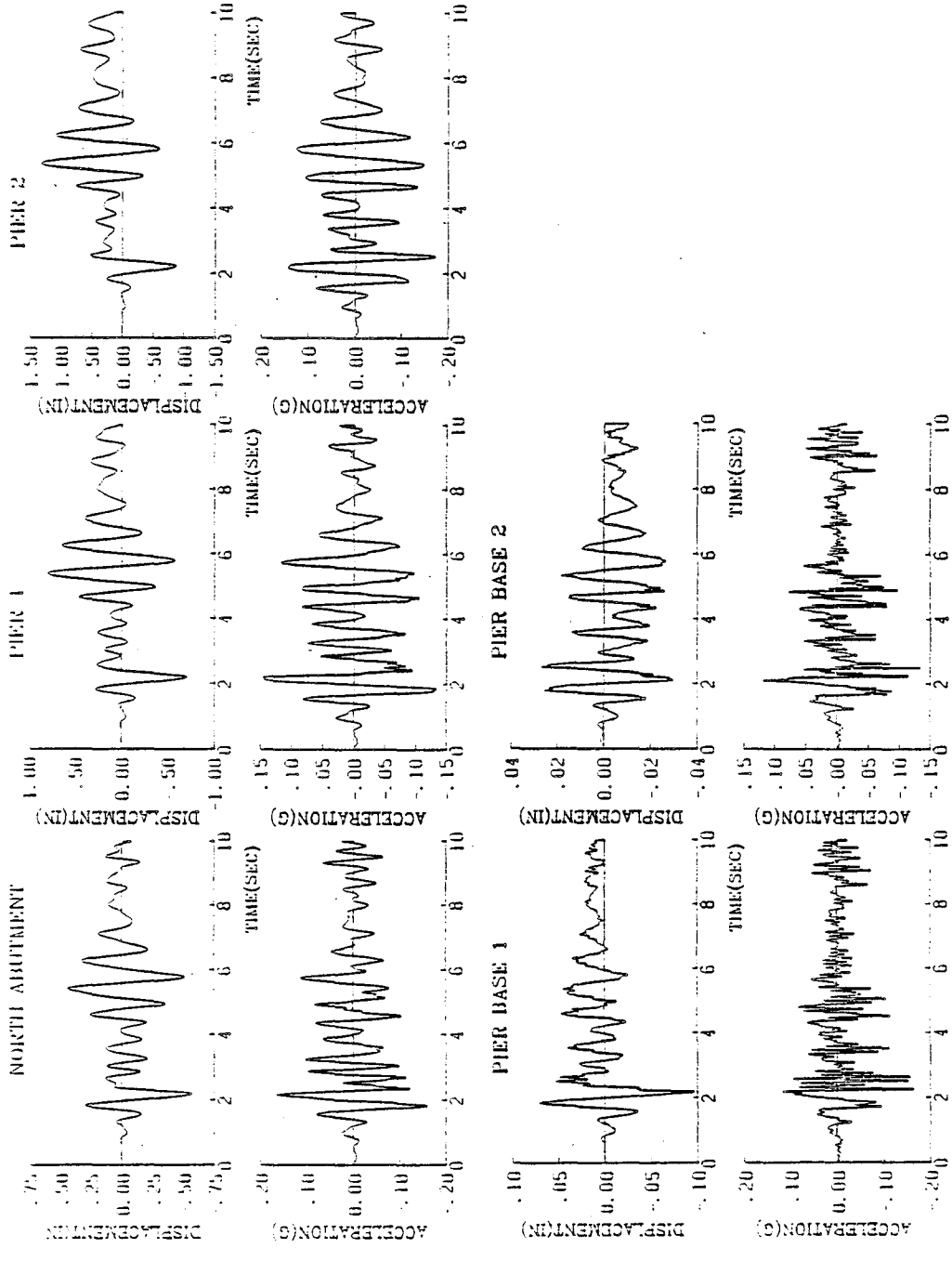

Fig. 6.3 Response Histories for El Centro NS with PGA = Ø.1g

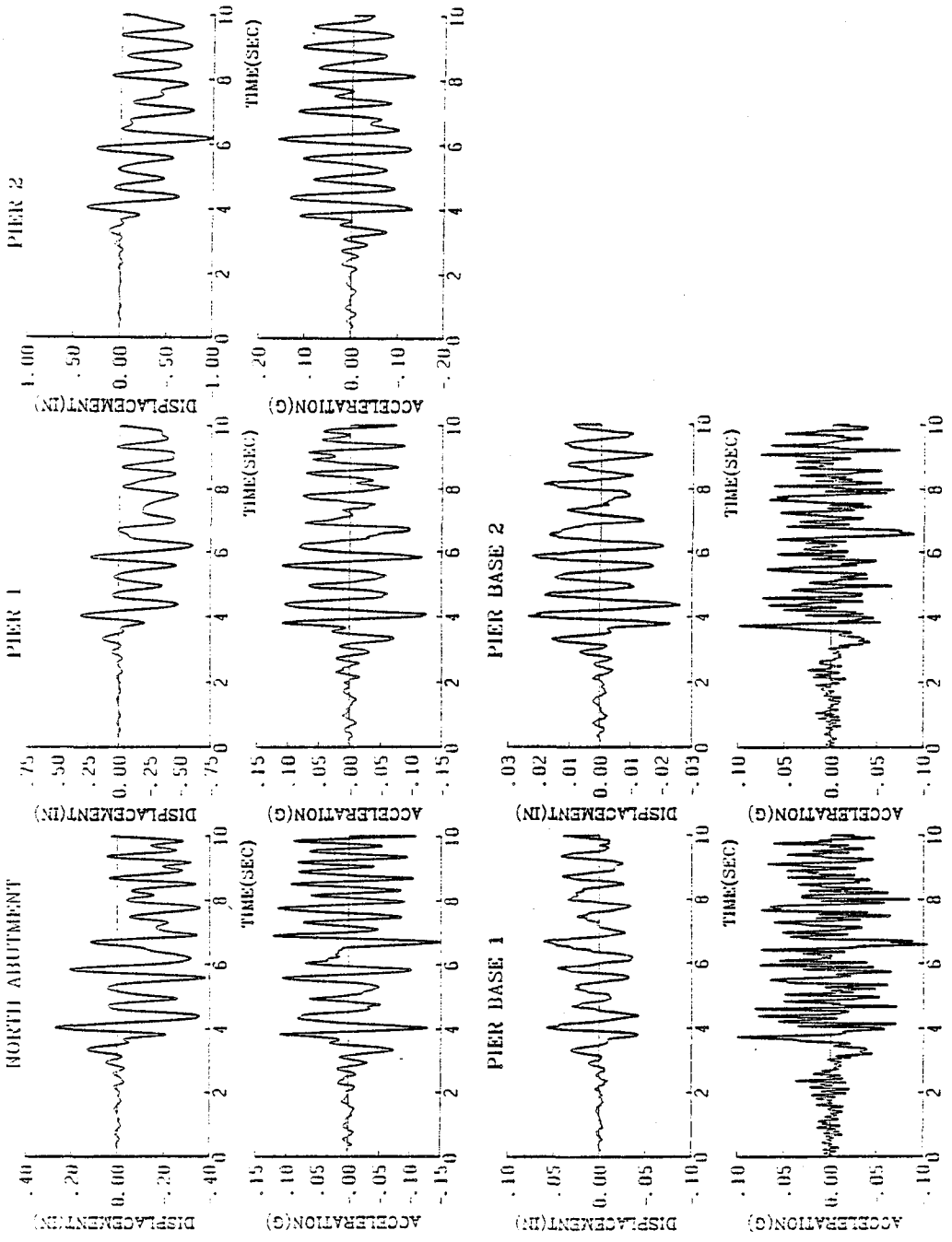

Fig. 6.4 Response Histories for Taft S69E with PGA = 0.1g

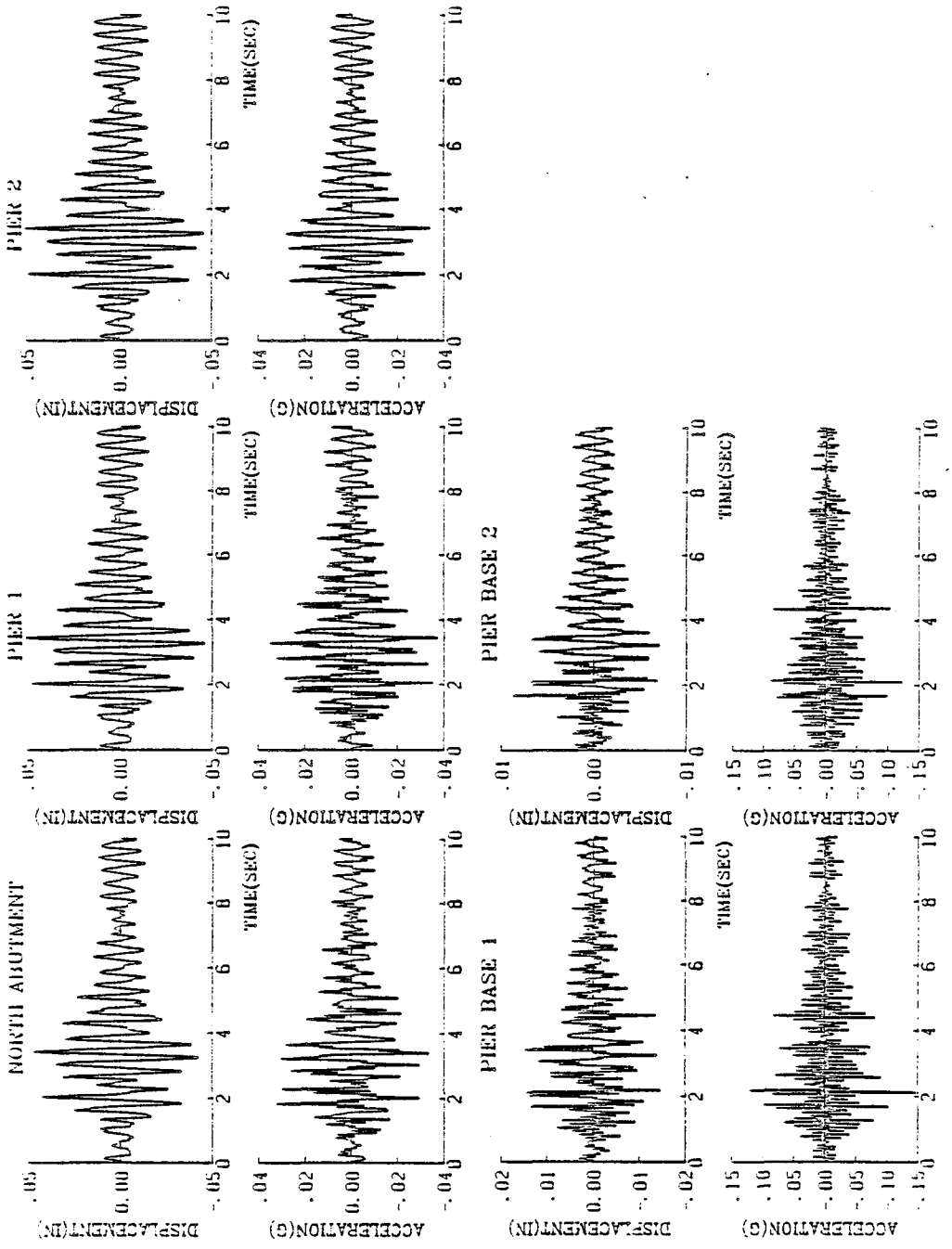

Fig. 6.5 Response Histories for Castaic N21E with PGA = 0.1g

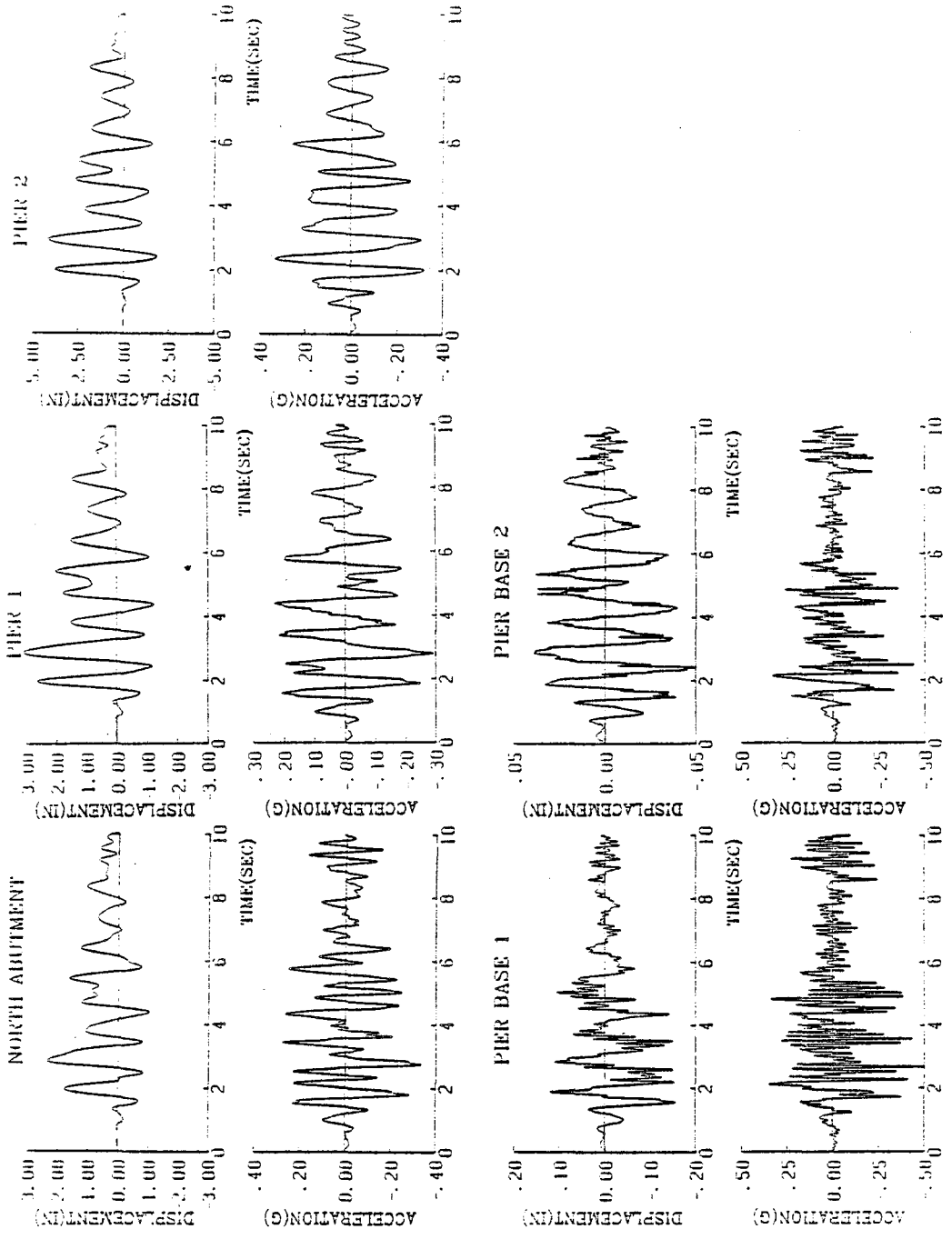

Fig. 6.6 Response Histories for El Centro NS with PGA = 0.35g

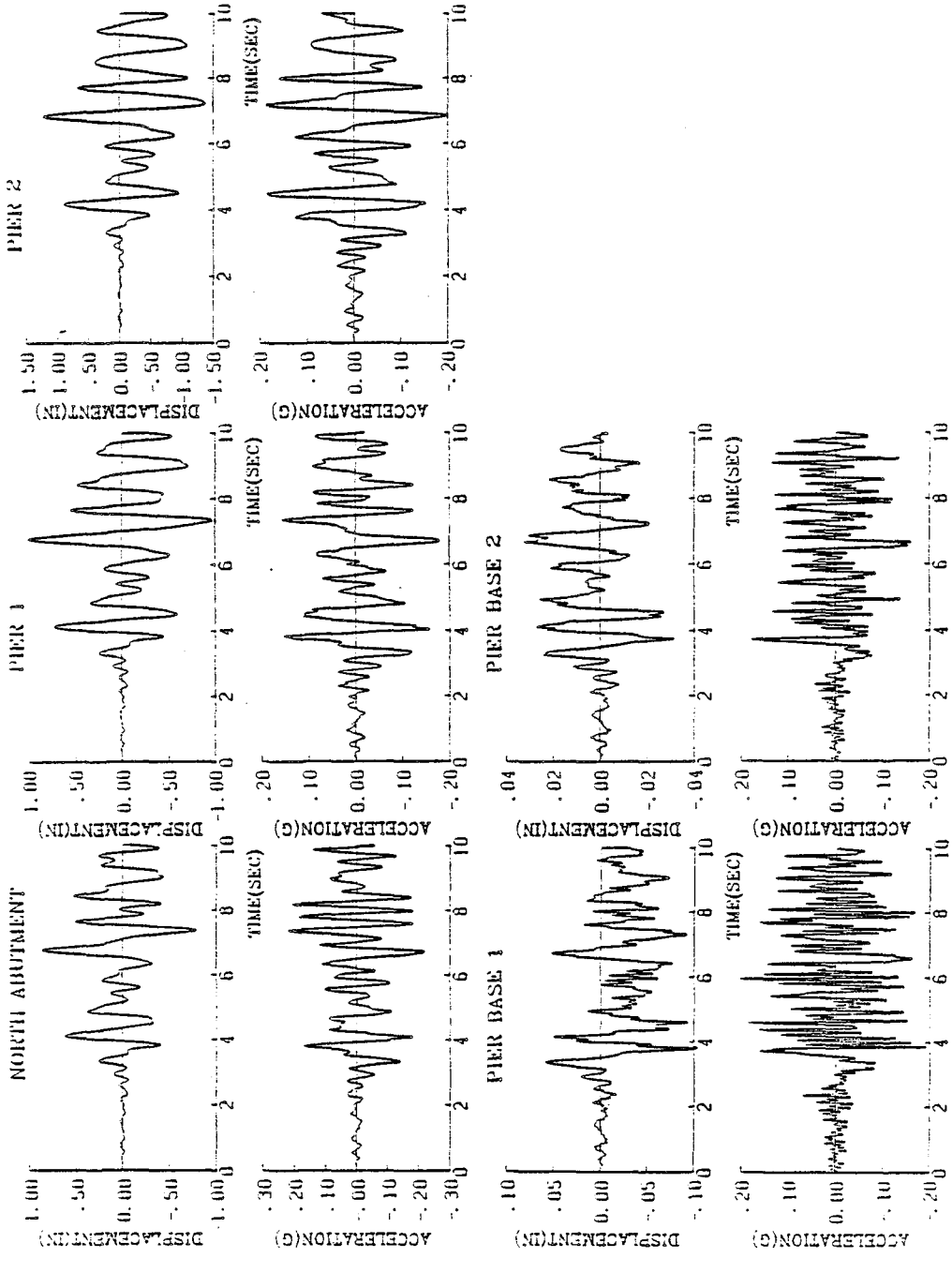

Fig. 6.7 Response Histories for Taft S69E with PGA = 0.18g

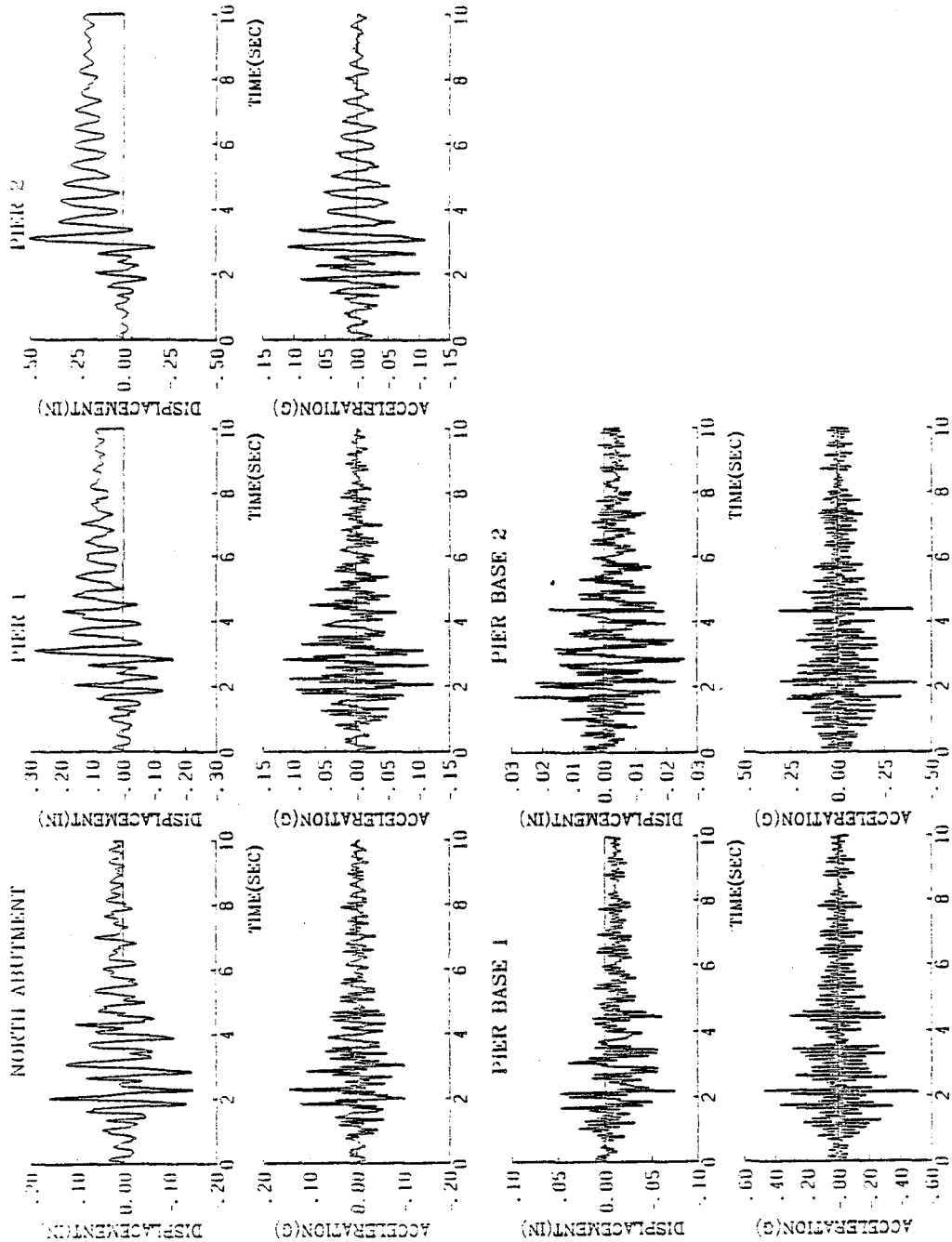

Fig. 6.8 Response Histories for Castaic N21E with PGA = 0.35g

APPENDIX A

NOTATIONS

The following symbols have been used in this report:

A = effective shear area;

D = deformation;

D_o = deformation at largest excurison point;

E = modulus of elasticity of concrete;

F = force;

F_o = force at largest excursion point;

f_B = flexibility of rotation spring;

G = concrete shear modulus; also, nonlinearity parameter in Ramberg-Osgood model;

I = moment of inertia;

J = torsional inertia;

K = stiffness;

L = element length;

M_c, M_y, M_u = cracking, yield, and ultimate moments at the column weak section, respectively;

θ_c, θ_y, θ_u = rotation at cracking, yield, and ultimate, respectively;

ϕ_y, ϕ_u = yield and ultimate curvatures, respectively.

APPENDIX B

UNIT CONVERSION FACTORS

To convert from ...	to ...	multiply by ...
inch	millimeter	25.4
foot	meter	Ø.3Ø48
kip-force	newton	4448
inch-kip-force	Kilonewton-meter	Ø.113Ø
kip/sq.inch	megapuscal (MPa)	6.895
pound-mass	kilogram	Ø.4536

APPENDIX C

LIST OF CENTER FOR CIVIL ENGINEERING EARTHQUAKE RESEARCH (CCEER) PUBLICATIONS

Report No.	Publication
CCEER-84-Ø1	Saiidi, Mehdi and Renee A. Lawver, "User's Manual for LZAK-C64, A Computer Program to Implement the Q-Model on Commodore 64," Civil Engineering Department, Report No. CCEER-84-Ø1, University of Nevada, Reno, January 1984.
CCEER-84-Ø2	Douglas, Bruce M. and Toshio Iwasaki, "Proceedings of the First USA-Japan Bridge Engineering Workshop," held at the Public Works Research Institute, Tsukuba, Japan, Civil Engineering Department, Report No. CCEER-84-Ø2, University of Nevada, Reno, April 1984.
CCEER-84-Ø3	Saiidi, Mehdi, James D. Hart, and Bruce M. Douglas, "Inelastic Static and Dynamic Analysis of Short R/C Bridges Subjected to Lateral Loads," Civil Engineering Department, Report No. CCEER-84-Ø3, University of Nevada, Reno, July 1984.